CHEMICAL SYSTEMS LABORATORY TECHNICAL REPORT

ARCSL-TR-80004

INFRARED TRANSMISSION THROUGH SCREENING SMOKES: EXPERIMENTAL CONSIDERATIONS

by

Gerald C. Holst

Research Division

May 1980

US ARMY ARMAMENT RESEARCH AND DEVELOPMENT COMMAND
Chemical Systems Laboratory
Aberdeen Proving Ground, Maryland 21010

Disclaimer

The findings in this report are not to be construed as an official Department of the Army position unless so designated by other authorized documents.

Disposition

Destroy this report when it is no longer needed. Do not return it to the originator.

UNCLASSIFIED

SECURITY CLASSIFICATION OF THIS PAGE *(When Data Entered)*

REPORT DOCUMENTATION PAGE

READ INSTRUCTIONS BEFORE COMPLETING FORM

1. REPORT NUMBER: ARCSL-TR-80004

2. GOVT ACCESSION NO.:

3. RECIPIENT'S CATALOG NUMBER:

4. TITLE *(and Subtitle)*: INFRARED TRANSMISSION THROUGH SCREENING SMOKES: EXPERIMENTAL CONSIDERATIONS

5. TYPE OF REPORT & PERIOD COVERED: Technical Report, August 1978–August 1979

6. PERFORMING ORG. REPORT NUMBER:

7. AUTHOR(s): Gerald C. Holst

8. CONTRACT OR GRANT NUMBER(s):

9. PERFORMING ORGANIZATION NAME AND ADDRESS: Commander/Director, Chemical Systems Laboratory, ATTN: DRDAR-CLB-PS, Aberdeen Proving Ground, Maryland 21010

10. PROGRAM ELEMENT, PROJECT, TASK AREA & WORK UNIT NUMBERS: Project 1L162622A554

11. CONTROLLING OFFICE NAME AND ADDRESS: Commander/Director, Chemical Systems Laboratory, ATTN: DRDAR-CLJ-R, Aberdeen Proving Ground, Maryland 21010

12. REPORT DATE: May 1980

13. NUMBER OF PAGES: 55

14. MONITORING AGENCY NAME & ADDRESS *(if different from Controlling Office)*:

15. SECURITY CLASS. *(of this report)*: UNCLASSIFIED

15a. DECLASSIFICATION/DOWNGRADING SCHEDULE: NA

16. DISTRIBUTION STATEMENT *(of this Report)*

Approved for public release; distribution unlimited.

17. DISTRIBUTION STATEMENT *(of the abstract entered in Block 20, if different from Report)*

18. SUPPLEMENTARY NOTES

19. KEY WORDS *(Continue on reverse side if necessary and identify by block number)*

Infrared	Thermal clutter	FLIR
Smoke	Transmissometer	Forward looking infrared system
Obscuration	Laser	
Infrared transmission	Thermal imaging systems	

20. ABSTRACT *(Continue on reverse side if necessary and identify by block number)*

Presented are the basic principles that the experimentalists should consider before measuring the infrared transmission of an aerosol. Three basic methods are examined: laser transmissometers, broadband radiometer-transmissometers, and thermal imaging systems. The effects of single and multiple scattering and receiver field of view are discussed. Aerosol coagulation and sedimentation are considered. The effects of the spectral properties of the detector response, atmospheric transmission, and source temperature are related to the measured

(Continued on reverse side)

DD FORM 1 JAN 73 1473 EDITION OF 1 NOV 65 IS OBSOLETE

UNCLASSIFIED

SECURITY CLASSIFICATION OF THIS PAGE *(When Data Entered)*

20. ABSTRACT (Contd)

transmission. This can differ significantly from the true aerosol transmission. When using a thermal imaging system, the amount of smoke necessary to obscure a target depends upon whether the thermal system has an automatic gain control. Furthermore the amount of smoke necessary depends upon the angular subtense of the target. All of experimental problems discussed are shown graphically in three flow charts.

PREFACE

The work described in this report was authorized under Project 1L162622A554, Chemical Munitions and Chemical Combat Support. This work was started in September 1978 and completed in September 1979.

The use of trade names in this report does not constitute an official endorsement or approval of the use of such commercial hardware or software. This report may not be cited for purposes of advertisement.

CONTENTS

LIST OF FIGURES

TABLE

INFRARED TRANSMISSION THROUGH SCREENING SMOKES: EXPERIMENTAL CONSIDERATIONS

I. INTRODUCTION.

In order to evaluate the effect of tactical screening smokes on infrared transmission, it is necessary to understand the complex interactions among many variables. The transmission depends upon the bulk properties of the material (e.g., index of refraction), as well as the particle-size distribution, concentration, and pathlength. The measured or apparent transmission can be quite different from true transmission because several simple basic facts are often overlooked. Therefore, it becomes quite difficult to compare data from different laboratories or from field tests because the experimental methodology is different at each location although data from any one particular laboratory may appear self-consistent. The variability in the grouped data (all laboratories) may be extremely high due to the methodology. In fact, the data in each laboratory may be so repeatable that each claims the other is in error.

In principle, it is possible to calculate the transmission of the smoke if the particle-size distribution, concentration, and pathlength, and the complex index of refraction are known. But these parameters are not always known precisely, and one resorts to experimentation to define them. The experiment becomes that of introducing a smoke with unknown infrared properties between the target and the detector. The ratio of the signal received with smoke to that without smoke is taken as the transmission.

In addition to transmissometers, the effects of screening smokes on thermal imaging systems is of interest. The experiment is similar to the transmissometer test. A smoke is introduced until the target can no longer be perceived by an observer. The amount of smoke required is a measure of the smoke's obscuring power. A second type experiment consists of introducing a "standard" smoke between several different imaging systems and a target. The concentration is increased until the target has disappeared on several imaging systems. At this point, certain conclusions are drawn about the smoke's screening effectiveness, but the results may be a measure of the system's behavior and the observer's ability rather than the smoke's effectiveness.

Presented in sections II through VII are the basic principles that the experimentalist should consider before designing the experiment. Although Beer's transmission law is appropriate for most situations, scattered light can increase the detected signal.

As shown in section II, by decreasing the detector's field of view (FOV), the scattered light can be minimized so that the measured transmission will be representative of the true transmission. When using Beer's law, it is tacitly assumed that the particle-size distribution is not changing. Any dynamic process such as coagulation or sedimentation can significantly affect the applicability of Beer's law.

For broadband detectors, the measured transmission depends upon the atmospheric transmission, target temperature, detector spectral response, and the smoke's spectral transmission. It is impossible to separate these factors from transmission data unless every

parameter is carefully measured and specified (section III). In the infrared, the cloud can attenuate the target signature, emit radiation if hot, and reflect radiation from other sources. In section IV, a detailed analysis is given on how to separate these various detected signals.

Thermal imaging systems operate differently from transmissometers. For a target to disappear from the screen, its signature must be below the equivalent noise level. This noise level depends upon the target angular subtense (section V). Furthermore, there are two distinctly different types of thermal imaging systems. How each of these operates and how a smoke may obscure a target for each is given in section VI. In addition to attenuating the target signature, a smoke may contain random hot spots which lead to thermal clutter. Clutter can confuse the observer and lead to false target detection. Since random clutter is difficult to analyze, a simplified case (large hot cloud obscuring a portion of the FOV) is presented in section VII.

Finally, all of the possible errors that may occur during experiments are shown in three flow charts.

II. LASER TRANSMISSION AND SCATTERING.

Using Beer's law (also called Bouguer's and Beer-Lambert law), it is possible to calculate the transmission of an aerosol when the mass extinction coefficient a, the concentration C, and the pathlength L are known:

$$T = \exp\left[-\int_0^L aC(\ell)d\ell \right] \tag{1}$$

Although C and L are physical quantities that can be easily changed, a is a function of the material and the particle-size distribution and shape. Assuming spherical particles, a can be calculated from the Mie scattering theory:

$$a = \frac{3}{4\rho} \int_r Q\left(m, \frac{r}{\lambda}\right) \frac{N(r)}{r} dr \tag{2}$$

where Q is the Mie scattering efficiency factor, m is the complex index of refraction, r is the radius of aerosol particle, λ is the wavelength, and N(r) is the number density size distribution. The reason that a is usually obtained experimentally is that often neither m nor N(r) is known. a can be calculated using equation 1 with the experimentally obtained values T, C, and L. From equation 2, it follows that, if the size distribution changes, then a will change also. Any dynamic process, such as coagulation, sedimentation, or introduction of a new aerosol with a different size distribution, will change N(r). For hygroscopic smokes, such as phosphorus and HC, the size distribution will depend upon the relative humidity and, hence, a will be a function of relative humidity.

In recent experiments, fog oil smoke was introduced into a large chamber (1.2 by 3.6 by 1.5 m high) by a vaporization condensation method. A laser transmissometer operating at

$\lambda = 0.6328\ \mu m$ measured the transmission (L = 1.2 m) as a function of time, as shown in figure 1. The concentration was simultaneously obtained, as shown in figure 2. This behavior is rather unusual because Beer's law states that, if the concentration is constant, as shown in the first 20 minutes of the experiment, then the transmission should also be constant.

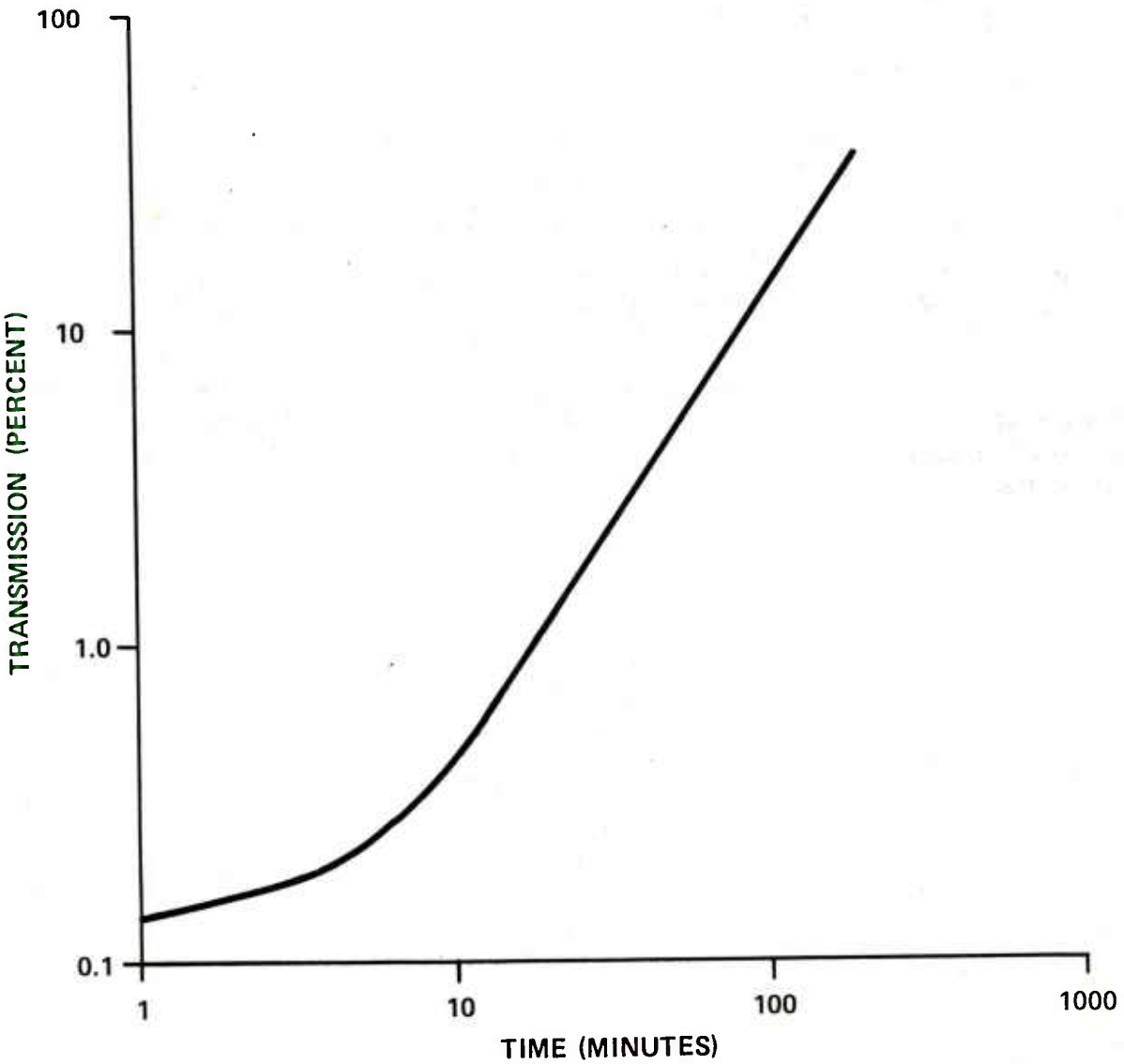

Figure 1. Transmission of a Fog Oil Smoke as a Function of Time

Data were obtained with a HeNe laser transmissometer ($\lambda = 0.6328\ \mu m$). Chamber size was 1.2 by 3.6 by 1.5 m high. Laser pathlength was 1.2 m. Since the transmission is changing with time, some type of dynamic process is occurring.

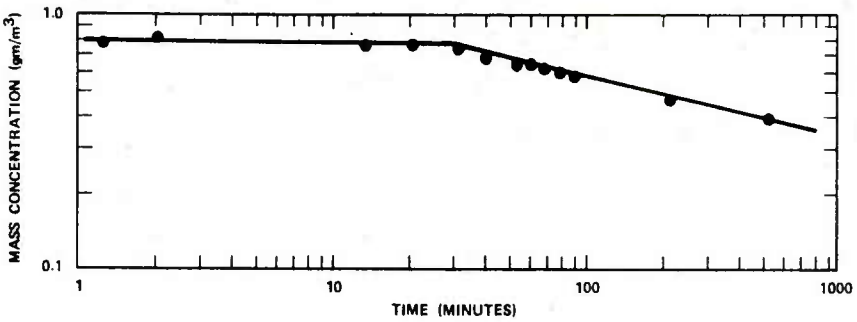

Figure 2. Mass Concentration of a Fog Oil Smoke as a Function of Time

Data were obtained by gravimetric analysis of glass fiber filters. The aerosol was aspirated for 1 minute for each sample. The aerosol is stable for the first 20 minutes before sedimentation takes place.

Fortunately, the answer lies in the size distribution. The distribution was obtained with cascade impactors at time t = 0.0 min and t = 51 min. As shown in figure 3, the total number of particles greater than 2.0 μm actually increased, indicating that significant coagulation has occurred.

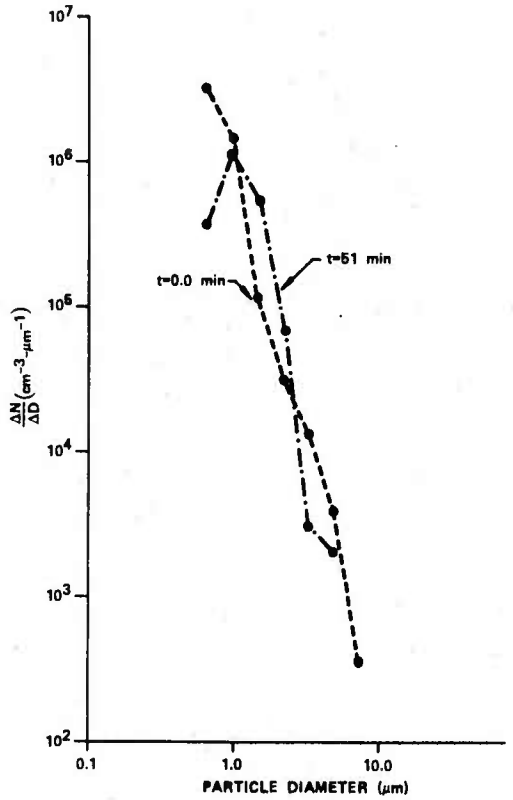

Figure 3. Particle-Size Distribution Obtained at t = 0 and t = 51 Minutes for a Fog Oil Smoke

Data were obtained from cascade impactors. This shift in the mode diameter is characteristic of coagulation.

Using the data in figures 1 and 2, the extinction coefficient was calculated and is plotted in figure 4. We see that a is a function of time because N(r) is a function of time also.

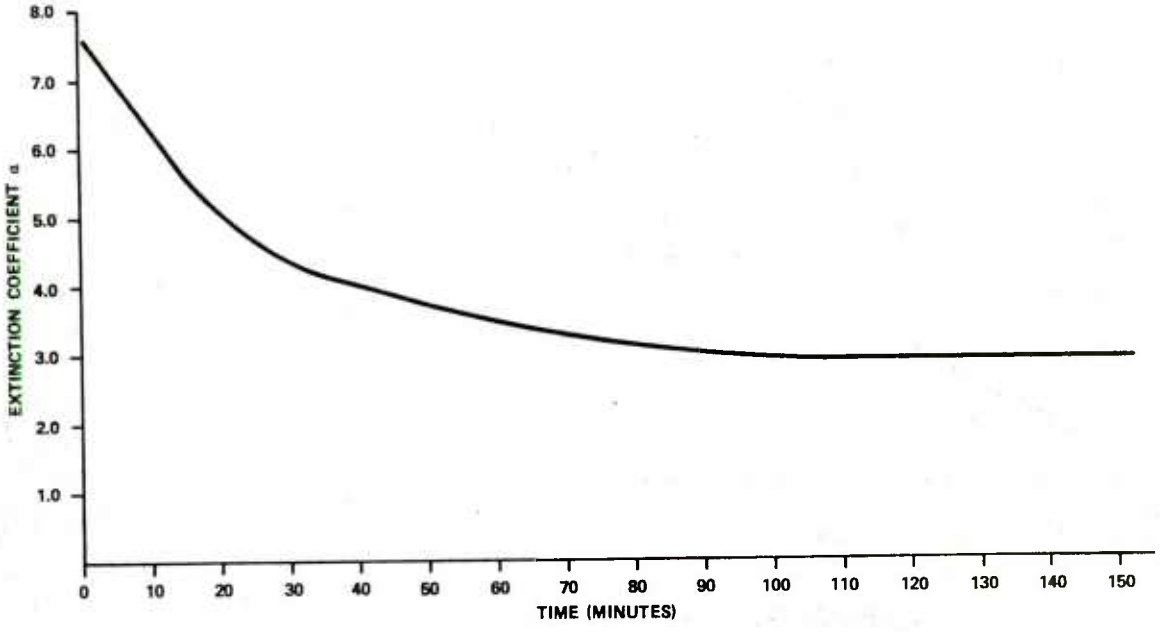

Figure 4. Calculated Extinction Coefficient as a Function of Time for a Fog Oil Smoke

The transmission data shown in figure 1, the mass concentration data shown in figure 2, and the pathlength L = 1.2 m were used in Beer's law. Since a is a function of time, the age of the cloud is significant when specifying a.

As a general rule, coagulation becomes significant when the number density exceeds 10^6 particles/cm^3 and the diameter is less than 1 μm. Sedimentation, on the other hand, dominates when D $>$ 1 μm in a chamber.

The extinction coefficient derived from Mie theory calculations assumes that any light scattered out of the incident beam contributes to total extinction. These calculations generally assume that the incident beam is a plane parallel wave of infinite extent and that the detector FOV is essentially zero. Beer's law is always valid for zero FOV detectors. In reality, the detector FOV is finite and the total amount of light entering the detector will depend upon how much scattering has taken place. Middleton[1] has shown that even for the single scattering case the amount of detected scattered light increases significantly as the detector FOV increases. His results (figure 5) are not directly applicable to laser transmissometers but they do point out the importance of exactly knowing the limitations of the experimental setup. Zuev[2] did not give experimental details, but he showed that Beer's law is valid down to $T = 10^{-13}$ (figure 6). Although our fog oil smoke experiments show significant coagulation at $\tau = 6$, Zuev does not mention any dynamic changes, even up to $\tau = 30$.

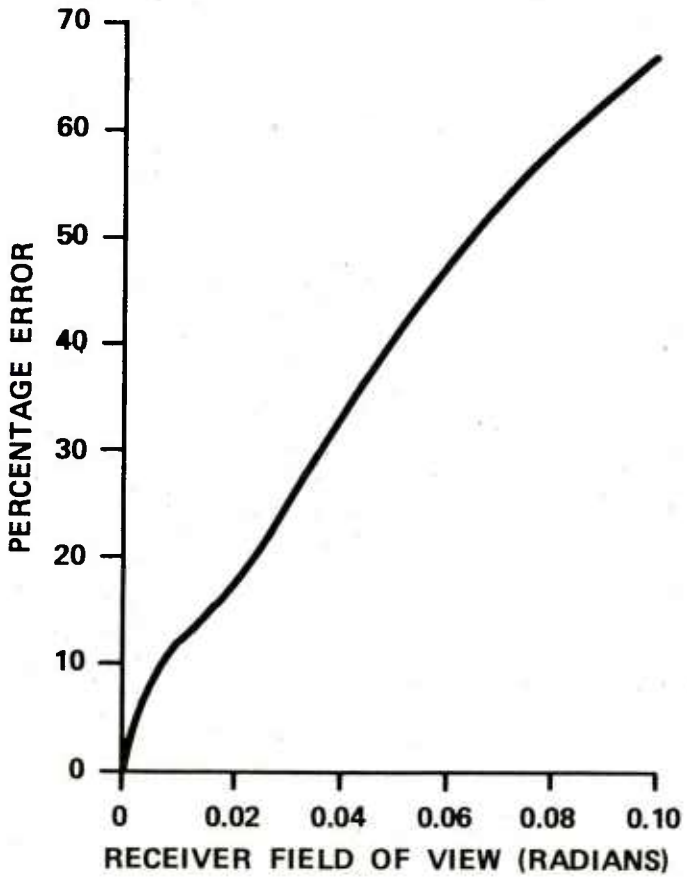

Figure 5. Calculated Percentage Error in Detected Signal as a Function of Receiver Field of View for a Water Fog (from Reference 1)

The percentage error is defined as the ratio of total detected light (direct and scattered) to the direct light only. The beam divergence was 2 radians; fog droplets were D = 5.0 μm, N = $10^2/cm^3$, $\alpha C = 3.93 \times 10^3$, and L = 1000 m.

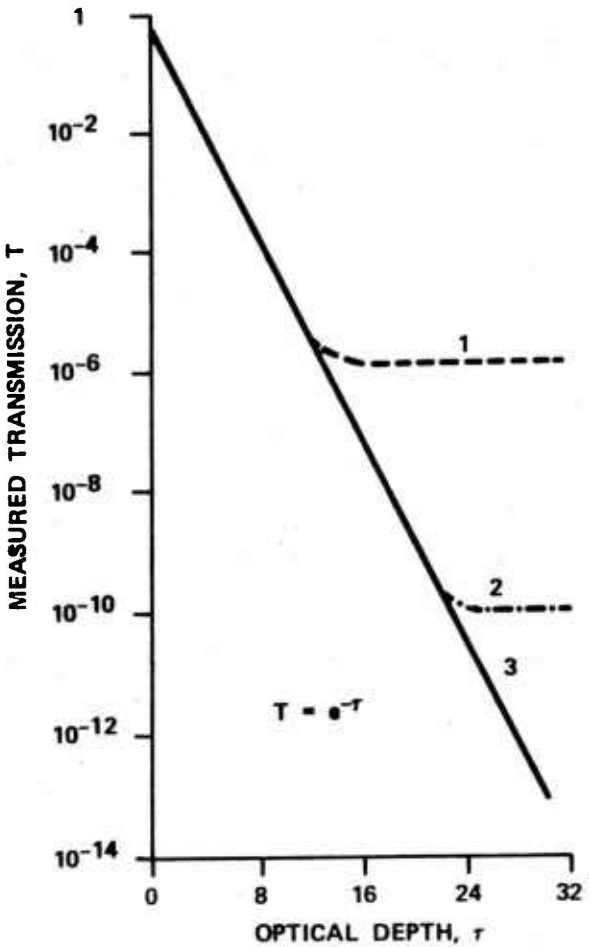

Figure 6. Measured Transmission as a Function of Optical Depth (from Reference 2)

Curve 1 is for dense lycopodium spores (D = 30 μm) suspended in alcohol in a small cuvette (L = 15 cm). The effects of multiple scattering become apparent for $\tau > 12$. For smoke (D = 1 to 2 μm) and artificial water fogs (D = 8 to 15 μm), curve 2 represents a situation where the laser and detector are side-by-side with the laser hitting a mirror 400 cm away. This is representative of all laser-induced detection and ranging (LIDAR) systems. Curve 3 is for a laser transmissometer operating over a 400-cm pathlength.

For dense aerosols, multiple scattering can occur. Second-order forward scattering has been heated theoretically.[3] The results indicate that, for typical polydisperse naturally occurring aerosols (Deirmendjian haze M, H, and C3), a correction factor can be applied to the measured transmission to obtain the true extinction. The factor

$$R = \frac{a_{\text{measured}}}{a_{\text{true}}} = \frac{a_\mu}{a_T} \tag{3}$$

appears in Beer's law as

$$T_{\text{meas}} = e^{-a_\mu CL} = e^{-Ra_\tau CL} \tag{4}$$

As shown in figure 7, this factor depends upon the receiver FOV and the size distribution. This correction factor has been formulated in a slightly different form[4] to account for all narrow-angle forward scattered light:

$$T = e^{-(aCL + D)} \tag{5}$$

where D is a function of the size parameter (r/λ), receiver FOV, and the divergence of the light beam. The values R and D have not been experimentally verified. Mooradian *et al.*[5] have shown that the detected signal is a function of receiver FOV for naturally occurring fogs. (See figure 8.)

The effects of multiple scattering are not limited to transmission measurements. The effects of second-order scattering on laser-induced detection and ranging (LIDAR) returns were considered theoretically by Eloranta.[6] It has been shown experimentally[7] that the backscatter signal increases as the receiver FOV increases. (See figure 9.)

Thus, the measured extinction depends upon the particle-size distribution, concentration, and pathlength, and the receiver FOV. Unless the precise relationship among these parameters is known, it is quite likely that the measured a will be different from the true a. Therefore, laboratories with different FOV's may obtain different extinction coefficients for the same smoke generated under identical environmental conditions. Any dynamic process that can alter the size distribution will affect a. The value of a obtained will depend on the age of the aerosol. Furthermore, since it may take several minutes to generate a smoke and to uniformly disperse it within a chamber, the time defined as $t = 0$ is rather arbitrary.

III. BROADBAND DETECTORS: SPECTRAL RESPONSE CONSIDERATION.

The extinction coefficient, as shown in equation 1, is, in general, a function of wavelength. For broadband detectors, the measured extinction is a function of the source temperature and the detector spectral response, as well as the spectral transmission of the smoke.

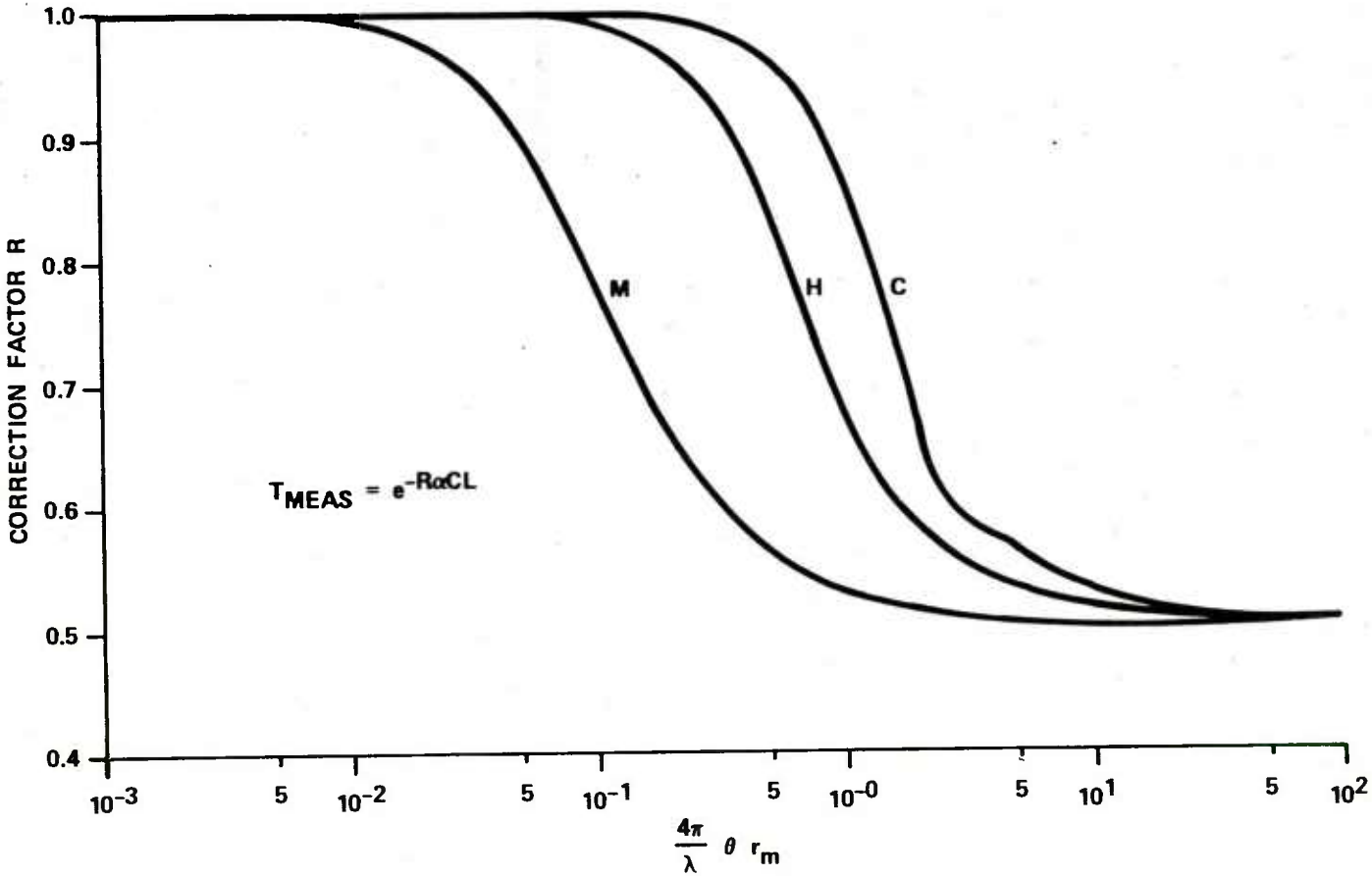

Figure 7. Correction Factor R as a Function of Experimental Geometry (from Reference 3)

M, H, and C refer to Deirmendjian haze models. λ is the wavelength of the laser transmissometer, θ is the receiver field of view, and r_m is the mode radius of the particle-size distribution. For a small field of view, no correction factor is needed (R = 1); whereas, for a large field of view, the correction is R = 0.5.

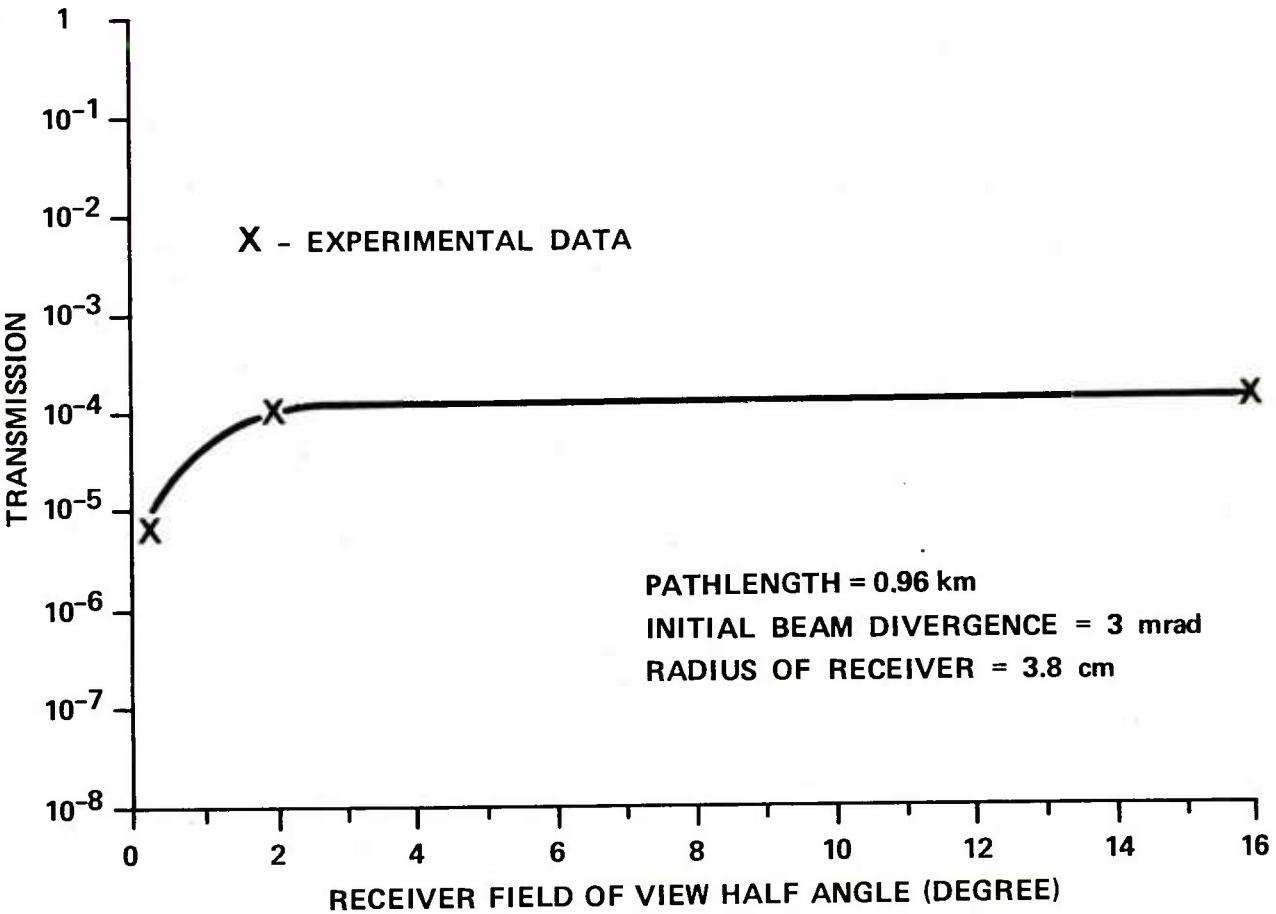

Figure 8. Measured Transmission as a Function of Receiver Field of View for Naturally Occurring Water Fogs (from Reference 5).

The optical depth $\tau = 11.8$. The fog was not homogeneous. The laser transmissometer was a frequency doubled Q-switched Nd:YAG laser ($\lambda = 0.53\ \mu m$). The solid line is the theoretical prediction which includes multiple scattering for dense aerosols.

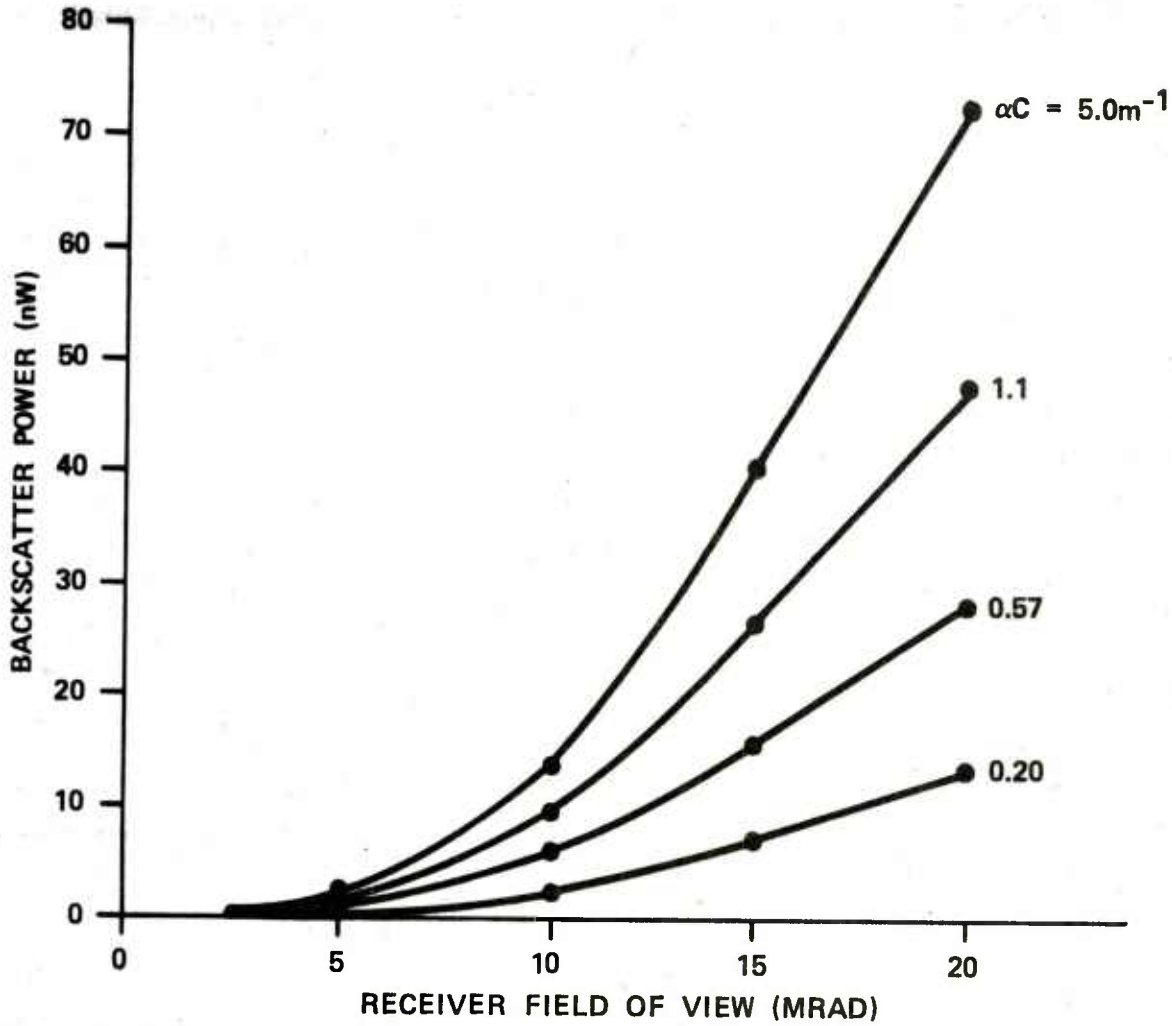

Figure 9. Detected Backscatter as a Function of Receiver Field of View (from Reference 7)

For dense artificial water droplet clouds as αC increases, the amount of backscatter light increases. An argon laser ($\lambda = 0.5145\ \mu m$) was used. In the limiting case of very dense aerosols, the amount of backscatter will be independent of optical depth. (See curve 2 in figure 6.)

The total flux detected depends upon the geometry of the scenario. Let us assume that this is fixed and that the detector's geometry is included in the calibration of the instrument. The flux reaching a detector from a target with emissivity ϵ_T at a single wavelength is given by

$$F_{OT} = \tau_a \epsilon_T R_T + L_a \tag{6}$$

where τ_a is the transmission of the intervening atmosphere, R_T is the blackbody power emitted by the target, and L_a is the radiance of the atmosphere. When an emissive smoke is introduced, the flux reaching the detector becomes

$$F_{ST} = \tau_s \tau_a \epsilon_T R_T + L_a' + \tau_a' R_s \tag{7}$$

where τ_s is the transmission of the smoke, L_a' is the radiance modified by the smoke, and τ_a' is the transmission of the atmosphere between the smoke and detector. R_s is a combination of the flux emitted by the smoke and the flux reflected off the cloud from external sources. This is the emission-reflection term.

The current signal generated by these fluxes is given by

$$I = SF \tag{8}$$

where S is the sensitivity of the detector. For broadband detectors, the detector integrates over the wavelength of interest so that

$$I = \int_\lambda SF d\lambda \tag{9}$$

All the parameters L_a, R, ϵ, and τ are in general a function of wavelength. With synchronous detection, the source is modulated at some frequency f and the detector electronics are sensitive to this frequency only. The path radiance and smoke emission are dc components and therefore are not measured. We assume that the smoke emission does not saturate the detector and that it is uniform over the entire FOV. The measured ratio of smoke to no-smoke currents becomes

$$\langle \tau \rangle = \frac{I_{ST}}{I_{OT}} = \frac{\int S \tau_s \tau_a \epsilon_T R_T d\lambda}{\int S \tau_a \epsilon_T R_T d\lambda} \tag{10}$$

where $\langle \tau \rangle$ is the mathematical average with respect to the function $S\tau_a\epsilon_T R_T$. It is the spectral averaged transmission and depends upon the spectral character of S, τ_a, R_T, and τ_s.

The effect of spectral mismatch between the smoke and the detector only is shown in the following exaggerated example. Consider four different hypothetical systems, all of which are nominally classified as 8- to 14-μm radiometer-transmissometer systems. The spectral sensitivity of each is shown in the table and depicted in figure 10. Assume that the geometry is identical for each detector and that scattering is not a factor, as described in section II.

Table. Spectral Sensitivity of Four "8- to 14-μm" Broadband Radiometer Systems

Detector	Spectral response*
	μm
1	8–14
2	11–14
3	8–12.5
4	8–11

* Relative response is 1.0 in these regions and zero elsewhere.

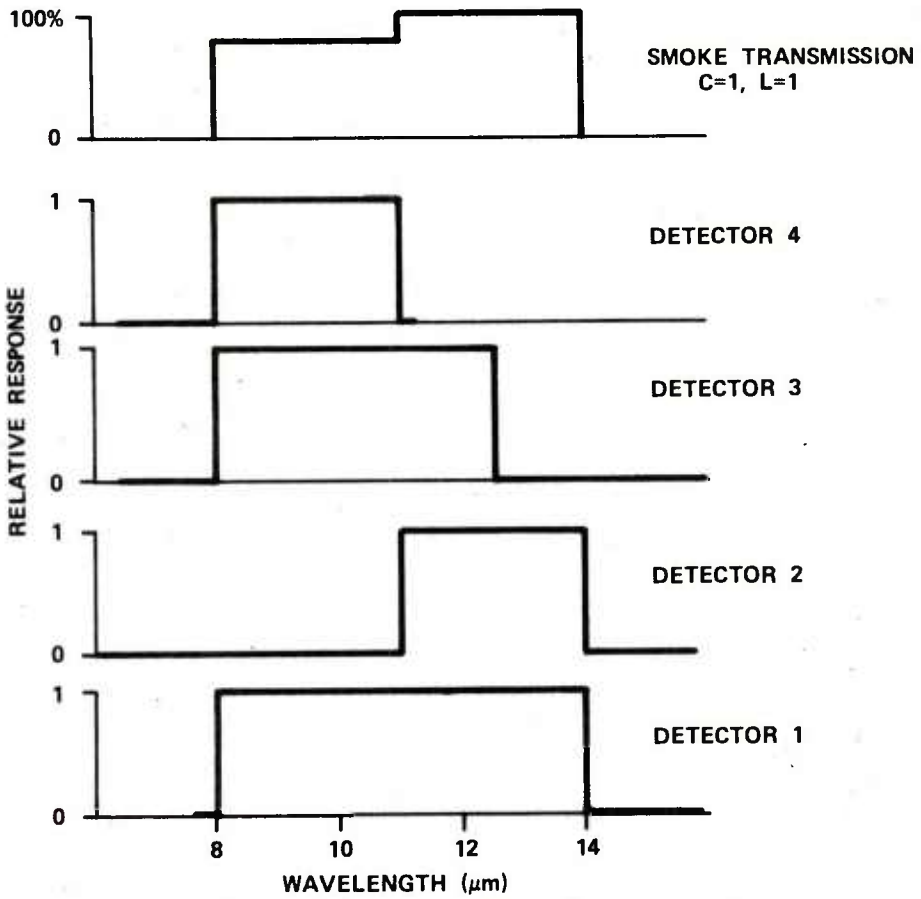

Figure 10. Spectral Response of Four Hypothetical Detectors

The relationship between these detectors and a hypothetical smoke is shown.

Consider a screening agent whose transmission is 80% from 8 to 11 μm and 100% from 11 to 14 μm for unit pathlength and unit concentration. As the smoke concentration increases, the transmission from 11 to 14 μm stays at 100%, and the transmission from 8 to 11 μm approaches zero. Thus, as far as detector 2 is concerned, the smoke is transparent. Since detector 1 integrates over the entire region, the transmission approaches 50% and, with detector 4, the transmission goes to zero. Detector 3 shows some intermediate value. In figure 11, the expected transmission for each of these detectors is plotted as a function of concentration. The values were calculated with equation 10 and by letting $R_T = \epsilon_T = \tau_a = 1$.

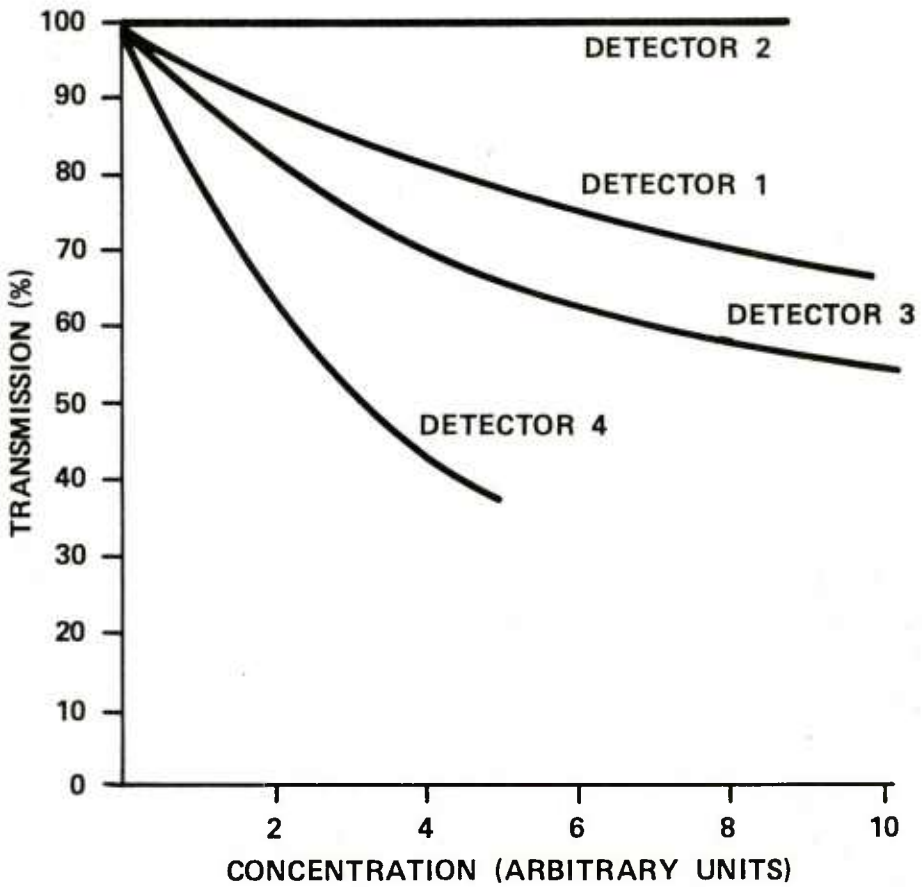

Figure 11. Calculated Transmission as a Function of Concentration.

The extremely large difference in transmission between detector 2 and detector 4 illustrates why spectral responses must be considered before collecting data.

A second way of comparing these systems is to calculate the apparent extinction as a function of concentration (figure 12). This representation is usually the method by which smokes are characterized experimentally. Suppose then a laboratory had the 8- to 14-μm transmissometer system with detector 1. After performing a series of experiments at several different concentrations (say C = 3, 4, 5, and 6) and performing a least-square fit to the experimental data, the laboratory would obtain an extinction coefficient of about 0.05. Another laboratory with another "8- to 14-μm" system with detector 2 would say the material was transparent.

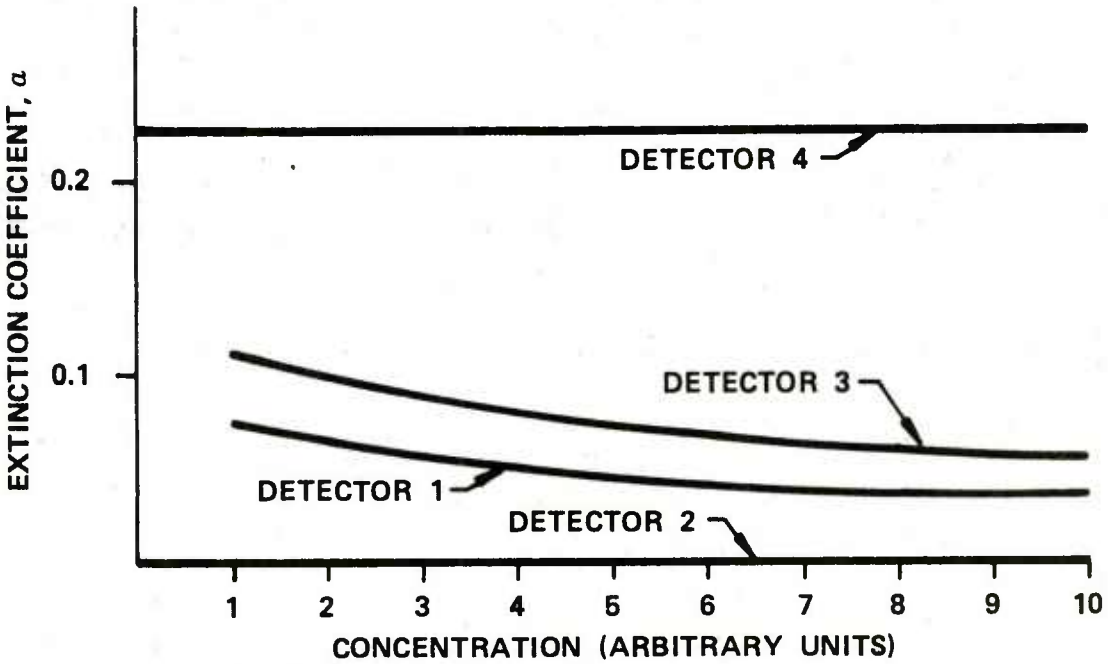

Figure 12. Calculated Extinction Coefficient as a Function of Concentration

The extinction coefficient, calculated from transmission data, for the four hypothetical detectors can vary dramatically depending upon the spectral response of the detector.

Although this example was exaggerated, the shape of the hypothetical smoke transmission is somewhat similar to phosphorus smoke.[8] It was pointed out by the author (appendix A) that different spectral response detectors can lead to different measured transmissions for the same concentration and pathlength.

The effect is not limited to the spectral mismatch of the smoke and detector. The spectral emission of the target (source) will also affect the measured transmission or extinction coefficient. Assuming that source is a blackbody, we have calculated the expected transmission for phosphoric acid smoke as a function of source temperature for a typical HgCdTe 8- to 14-μm detector (figure 13). We have included the effects of the atmosphere (relative humidity, 72%; pathlength, 400 m).

Thus it is easy to see that there is no simple way of obtaining the smoke transmission with a broadband detector because the measured transmission depends upon the target temperature, spectral response of the detector, and the atmospheric transmission. The atmospheric transmission is a function of pathlength, relative humidity, temperature, and local naturally occurring aerosols.

IV. AEROSOL EXTINCTION EMISSION-REFLECTION MEASUREMENTS.

In section III, it was assumed that the signal reaching the detector was modified only by the aerosol extinction. In this section, we consider three possibilities: (1) the smoke may be hotter than ambient and, therefore, may emit radiation; (2) the cloud may reflect

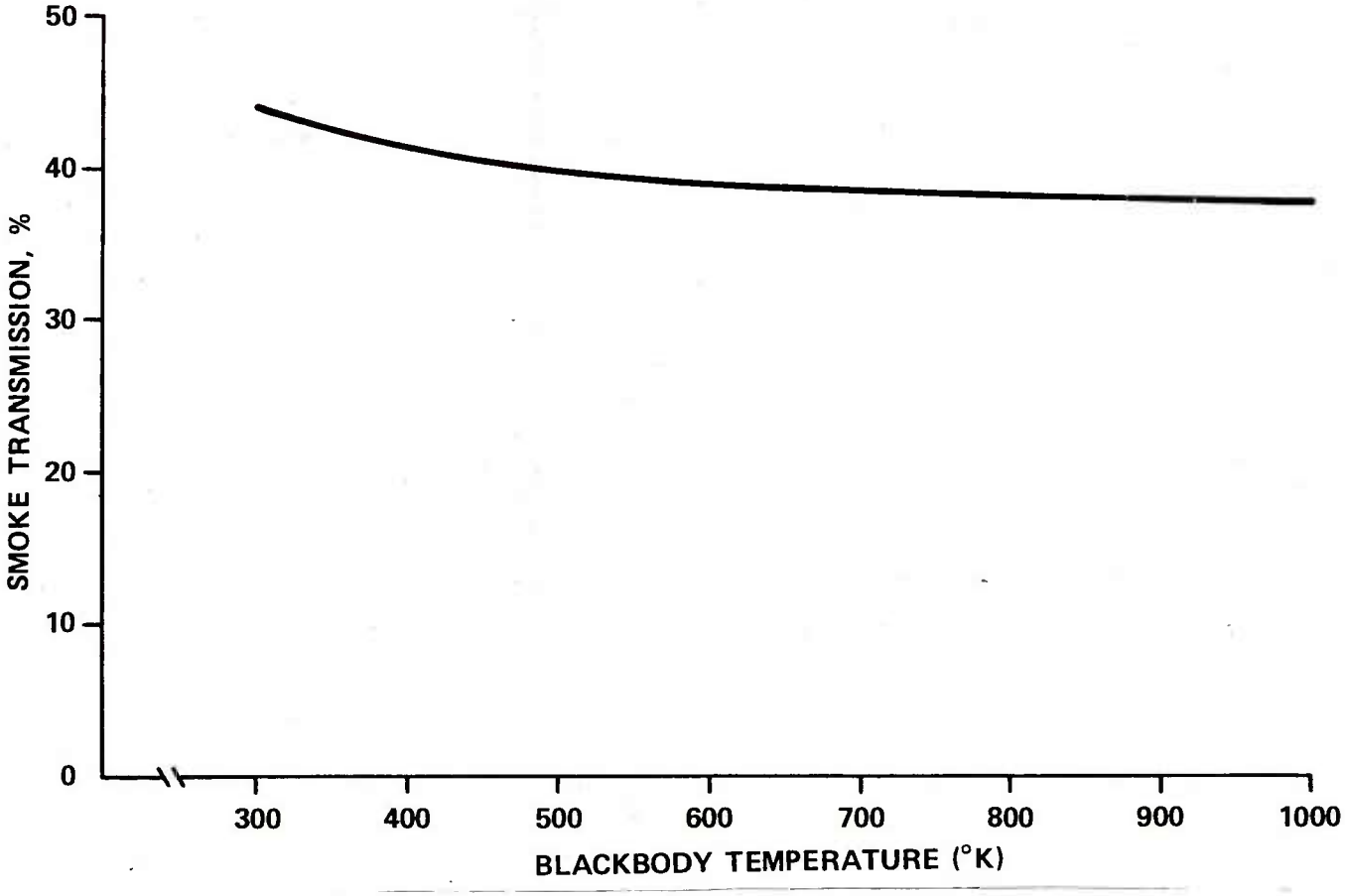

Figure 13. Expected Transmission of Phosphoric Acid Smoke Using a Typical HgCdTe Detector (8- to 14-μm) as a Function of Target Temperature

Atmospheric pathlength = 400 m, RH = 72%, and CL = 3.

radiation from external sources; and (3) the atmosphere itself may produce radiation. Note that, in field tests, the sun and earth are the external sources; whereas, in the laboratory, the chamber walls are the external sources. With care, it is possible to eliminate these effects.

There are two general methods available for separating extinction from emission, reflection, and path radiance. The first is synchronous detection, and the second is the use of two detectors: one that looks at the target and the other that looks at the background. The second method is equivalent to having a single detector that alternately looks at the target and background and is representative of all thermal imaging systems.

Synchronous detection was discussed in section III, and equation 10 gives the measured transmission.

If two light choppers are used, so that the source is modulated at frequency f_1 and the total flux reaching the detector is modulated at f_2, then we can extract both the transmission and reflection-emission properties of the smoke. The detector requires two tuned circuits: one sensitive to f_1 and another sensitive to f_2. Using equation 10, we obtain $\langle\tau\rangle$ from the circuit sensitive to f_1. The ratio of no smoke to smoke for the circuit sensitive to f_2 is

$$\left.\frac{I_{ST}}{I_{OT}}\right|_{f_2} = \frac{\int S(\tau_s \tau_a \epsilon_T R_T + L_a' + \tau_a' R_s) d\lambda}{\int S(\tau_a \epsilon_T R_T + L_a) d\lambda} \tag{11}$$

It is possible to separate the terms if several reasonable assumptions are made. If the atmosphere is at the same temperature as the background, then the path radiance can be neglected and

$$\left.\frac{I_{ST}}{I_{OT}}\right|_{f_2} = \langle\tau\rangle\Big|_{f_1} + \frac{\int S\tau_a' R_s d\lambda}{I_{OT}\Big|_{f_1}} \tag{12}$$

If narrow band detectors are used, then the emission-reflection term is obtained directly. Therefore, if we had a scanning spectrophotometer, we could obtain the entire spectral emission-reflection from the cloud.

If synchronous detection is not used, it is easy to see from equations 6 and 7 that there is no way in general of separating emission from transmission by a single measurement with broadband detectors. These effects can be minimized by judiciously choosing wavelengths, matching the receiver FOV and aperture to the source size and beam divergence, and using selective bandwidth filters. For laser transmissometers, extremely narrow bandwidth filters can be used; and, if external sources are minimized, transmission measurements can yield good data provided that all the precautions listed in section II are considered.

Let us consider the case where a second detector is allowed to look at the background (or alternately one detector scans the target and background as with a thermal imaging system). The flux reaching the detector due to the background is

$$F_{OB} = \tau_a \epsilon_B R_B + L_a \tag{13}$$

and with an emissive-reflective smoke this becomes

$$F_{SB} = \tau_s \tau_a \epsilon_B R_B + L_a' + \tau_a' R_s \tag{14}$$

If we measure the difference between the target and background, the ratio of smoke to no-smoke signals becomes (assuming $L_a = L_a'$)

$$\langle \tau' \rangle = \frac{I_{ST} - I_{SB}}{I_{OT} - I_{OB}} = \frac{\int S \tau_s \tau_a (\epsilon_T R_T - \epsilon_B R_B) d\lambda}{\int S (\epsilon_T R_T - \epsilon_B R_B) d\lambda} \tag{15}$$

Thus, for a two-detector system sensitive only to flux differentials, the detected signal does not depend upon the path radiance or the emissive-reflective properties of the smoke. The primary assumption is that the smoke is homogeneous and covers both the target and background uniformly. For smokes whose transmission is wavelength independent, then $\tau_s = \langle \tau' \rangle$. Note that the average transmission measured with a two-detector system is not the same as the average measured with synchronous detection. Both methods yield the true smoke transmission only if narrow band detectors are used.

As shown in all of the above equations, at a certain wavelength the current generated by the detector is proportional to the flux reaching the detector (equation 8). The total current generated is the integrated effect of the spectral response of the detector and the spectral emission of the source (equation 9). Since the source is usually a blackbody, the detector response is calibrated against the blackbody temperature. Note that the detector is not sensitive to the temperature directly but only to the flux reaching it. The relationship between photon emission and temperature is given by Planck's blackbody equation. Since this is not a linear relationship, the calibration of a detector is not linear. (See figure 14.) For convenience, the output is usually linearized about ambient temperature so that

$$I = I_o (1 + K \Delta T) \tag{16}$$

where I_o is the current generated by a blackbody source operating at ambient temperature. The difficulty with this relationship is that the current is related to the flux by equation 9. Introduction of a smoke with spectral character will alter the calibration (the constant K).

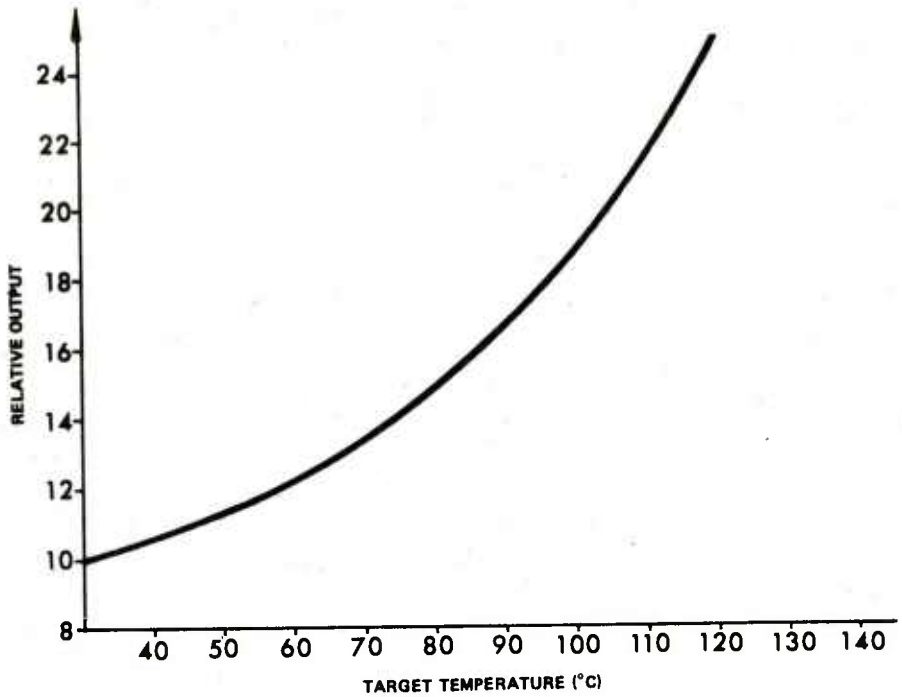

Figure 14. Typical Calibration Curve for an AGA Thermovision System

The output is calibrated as a function of the blackbody temperature.

As shown in appendix B, a more fruitful analysis which indicates the magnitude of errors introduced is to linearize the target output so that

$$R(T_o + \Delta T) = R(T_o)\,[1 + a\,\Delta T] \tag{17}$$

where $R(T_o)$ is the ambient blackbody flux evaluated at temperature T_o and at a single wavelength midpoint in the region of interest. Using this relationship in equations 10 and 15 and if $\epsilon_T = \epsilon_B$, it can easily be shown that

$$\langle \tau' \rangle = \langle \tau \rangle = \frac{\int S\tau_a\tau_s d\lambda}{\int S\tau_a d\lambda} \tag{18}$$

Although this result is what would be expected if equation 16 is used, the important difference is that mathematically we have linearized the flux reaching the detector rather than the calibration of the system. Smoke will attenuate only flux not the calibration. The ΔT analysis conforms to convention but can introduce significant errors. The magnitude of the errors is similar to that shown in section III. The use of the expansion also introduces errors but it conceptually makes sense.

The effects of atmospheric transmission is readily apparent in all of the equations shown. Since pathlengths are generally very short in the laboratory, τ_a is often neglected. However, in the field, the measured transmission is affected by τ_a and cannot be neglected. This again emphasizes the fact that broadband transmission measurements are confounded by the atmosphere, the target temperature, and the detector spectral sensitivity. Even though emission and reflection can be eliminated, broadband detectors at best can yield the spectral averaged transmission $<\tau>$.

V. IMAGING SYSTEMS: MINIMUM RESOLVABLE TEMPERATURE CONSIDERATIONS.

In section III, it was assumed that the broadband detector was calibrated so that the output could be displayed on some type of voltmeter. The imaging systems, in addition to having the same limitations as discussed in the preceding sections, also rely upon the observer's evaluation of the image. As mentioned when evaluating the effectiveness of a smoke, the smoke concentration is increased until an observer can no longer detect the target. At this point, the target signature is below the internal noise of the entire detector-electronics-human observer system.

The noise level is referred back to the input as an equivalent temperature and is specified as the minimum resolvable temperature (MRT) above ambient for a "standard" observer and is expressed as a temperature differential ΔT above ambient. The MRT is a function of the angular subtense a of the target and is plotted for two systems in figure 15. These systems are identical in the sense that for all targets larger than a_c they exhibit the same MRT. At another target angular subtense a_1, the MRT's of the two systems are given by ΔT_{N1} and ΔT_{N2}, respectively. Assume that a target is presented before these two systems and it is ΔT above the ambient. If an absorbing smoke is placed between the detectors and the target, then, since ΔT_1 is larger than ΔT_2, more smoke is needed to bring the target signature below the MRT for system 1 than for system 2.

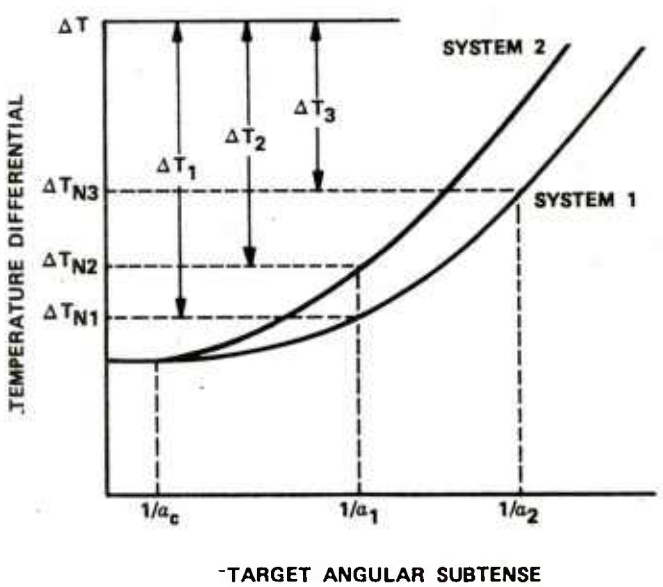

Figure 15. Minimum Resolvable Temperature of Two Hypothetical Imaging Systems as a Function of Target Angular Subtense

Consider instead that, during two different tests, only system 1 is used and the target sizes are slightly different (a_1 and a_2). Since ΔT_1 is greater than ΔT_3, more smoke is needed to obscure target size a_1. During field smoke trials, actual military targets (tanks, trucks, etc.) are used. The equivalent ΔT of the target depends upon the emissivity, target temperature, target size, and the spatial distribution of the heat (e.g., the engine area will be the hottest area). The equivalent ΔT is calculated so that the MRT can be used to describe system performance. Since the spatial distribution of the heat and the temperature can change from test to test, it is easy to see that the equivalent ΔT will change. Therefore, it becomes exceedingly difficult to compare field data. Conclusions reached about the effectiveness of smoke may result from differences in the detector MRT or target equivalent ΔT rather than the optical properties of the smoke.

In many field tests, trained observers are not used. The relationship between a trained observer and a casual observer is not clear. This is extremely important because the systems are characterized by how well a trained observer can perceive targets.

VI. TARGET OBSCURATION.

Consider, now, an imaging device which processes the detected flux into various gray levels to produce an image on a TV screen. Let us assume that the device is adjusted so that, before the smoke is introduced, the hot target will appear as pure white and the background will appear as black. Let us assume that the device will insert 10 gray levels between these points so that each gray level is given by

$$G = M \frac{I_{OT} - I_{OB}}{10} \tag{19}$$

where M is the electronic transfer function of the device.

Before any further analysis is possible, the exact mode of operation of the thermal imaging system must be known. There are two basic modes. In the first, the instrument is adjusted for optimum display and the controls are not further adjusted, even after the smoke is introduced. In the second mode, the internal automatic gain control (AGC) automatically adjusts the gain so that an optimum display is always present. The first mode is typical of laboratory-type systems and the second is typical of military imaging (forward looking infrared – FLIR) systems. Let us also consider the case where the smoke is homogeneous.

Let us first consider a device which will not be readjusted. There are three possible conditions which will obscure the target (figure 16):

CASE A. With strong attenuation and minimal emission-reflection, the target signature will be below the pure black level and the entire image on the screen will be black.

$$I_{ST} \leq I_{OB} \tag{20}$$

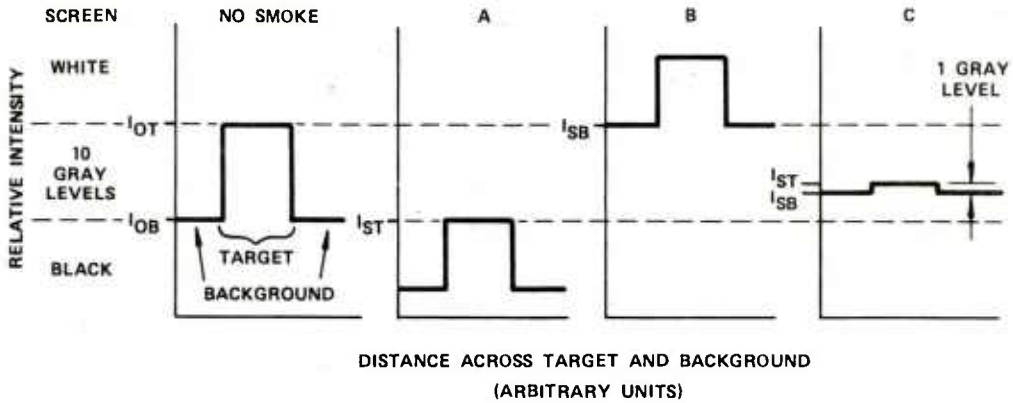

Figure 16. Three Methods of Obscuring a Target Detected with a Thermal Imaging System

With no smoke, the target is pure white and the background is pure black. In A, smoke reduced the target signature below the black level. In B, the smoke emission-reflection raised the background into the white level. In C, emission-reflection combined with attenuation put the target-background intensity differential into a gray level.

which results in

$$\int S(\tau_s \tau_a \epsilon_T R_T + L_a')d\lambda \leqslant \int S(\tau_a \epsilon_B R_B + L_a)d\lambda \tag{21}$$

If $L_a' \approx L_a$, then

$$\int S\tau_s \tau_a \epsilon_T R_T d\lambda \leqslant \int S\tau_a \epsilon_B R_B d\lambda \tag{22}$$

Using the linearization approximation (equation 17) and letting the emissivities be wavelength independent and using equation 10, we have

$$\langle \tau \rangle \leqslant \frac{\epsilon_B}{\epsilon_T} \left(\frac{1}{1 + a\,\Delta T} \right) \tag{23}$$

This is plotted in figure 17 for both the 3- to 5-μm and 8- to 14-μm regions. The graph shows that, with minimal emission-reflection, the transmission can be quite high and still drive the target signature below the background.

For the system that is not readjusted, the reason a relatively high transmission will obscure a target is that the flux differential between the target and background is very small.

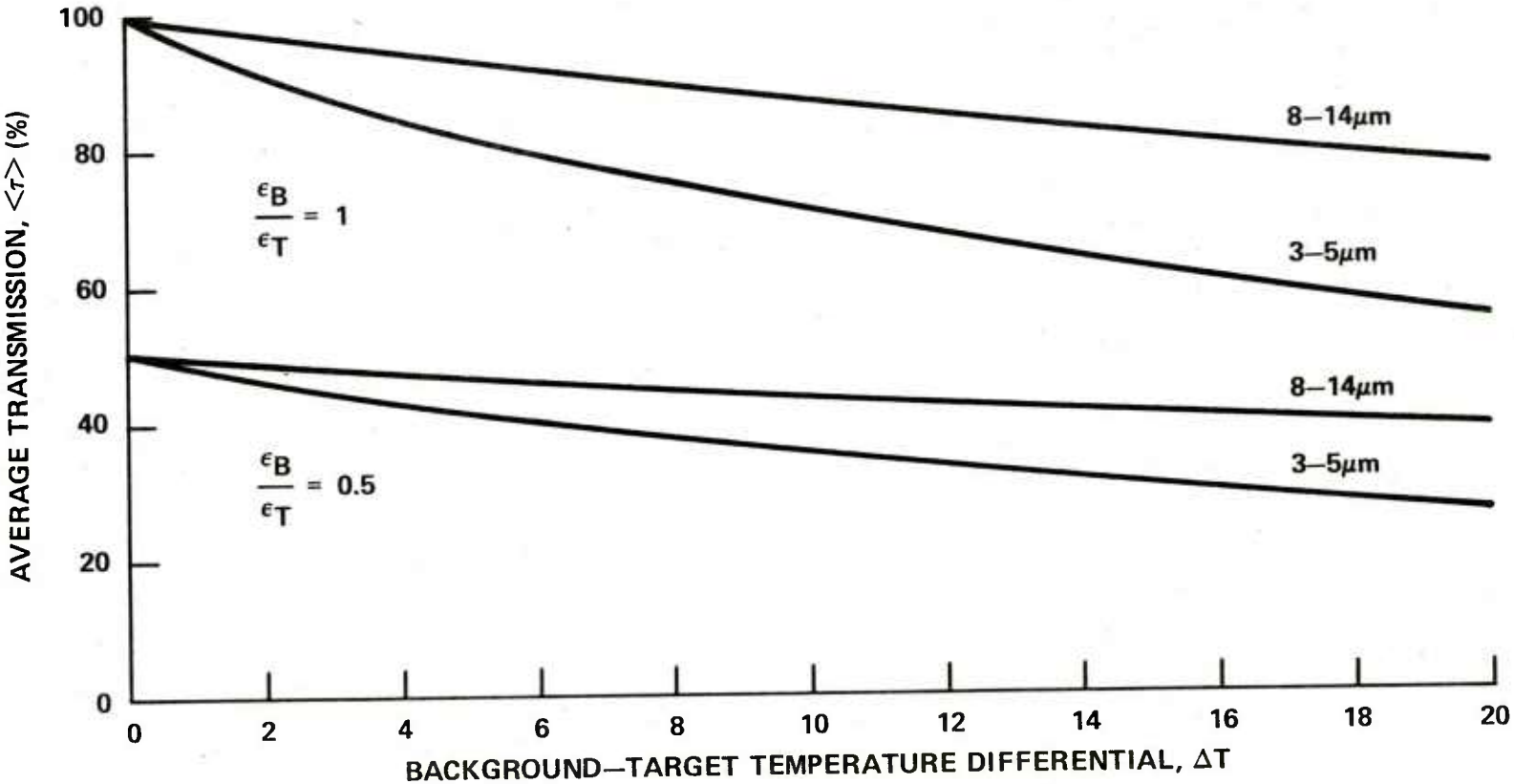

Figure 17. Average Transmission Necessary to Reduce the Target Signature below the Black Level (Case A)

CASE B. With strong emission-reflection, the apparent background signal (cloud plus background) will increase to the pure white level and the entire screen will be white

$$I_{SB} \geqslant I_{OT} \tag{24}$$

which results in

$$\int S(\tau_a \tau_s \epsilon_B R_B + \tau_a' R_s + L_a')d\lambda \geqslant \int S(\tau_a \epsilon_T R_T + L_a)d\lambda \tag{25}$$

If $L_a' \simeq L_a$ and $\tau_a' = \tau_a$

$$\int S\tau_a(\tau_s \epsilon_B R_B + R_s)d\lambda \geqslant \int S\tau_a \epsilon_T R_T d\tau \tag{26}$$

If we equate the emission-reflection flux to some equivalent blackbody temperature ΔT_s above the background with emissivity ϵ_s and if the emissivities are wavelength independent, then

$$\Delta T_s \geqslant \frac{(1 + a\,\Delta T)\,\epsilon_T - \langle\tau\rangle\,\epsilon_B - 1}{\epsilon_s a} \tag{27}$$

If we allow $\epsilon_T = \epsilon_B = 1$, then

$$\Delta T_s \geqslant \frac{1}{\epsilon_s}\left[\Delta T - \frac{\langle\tau\rangle}{a}\right] \tag{28}$$

For $\epsilon_s = 1$, this is plotted in figure 18 for both the 3- to 5-μm and 8- to 14-μm systems. The negative ΔT_s indicates that the cloud can be colder than the background to drive the background plus cloud signal into the pure white range. This is rather interesting for it indicates that it does not require much energy (flux) to saturate a system without AGC.

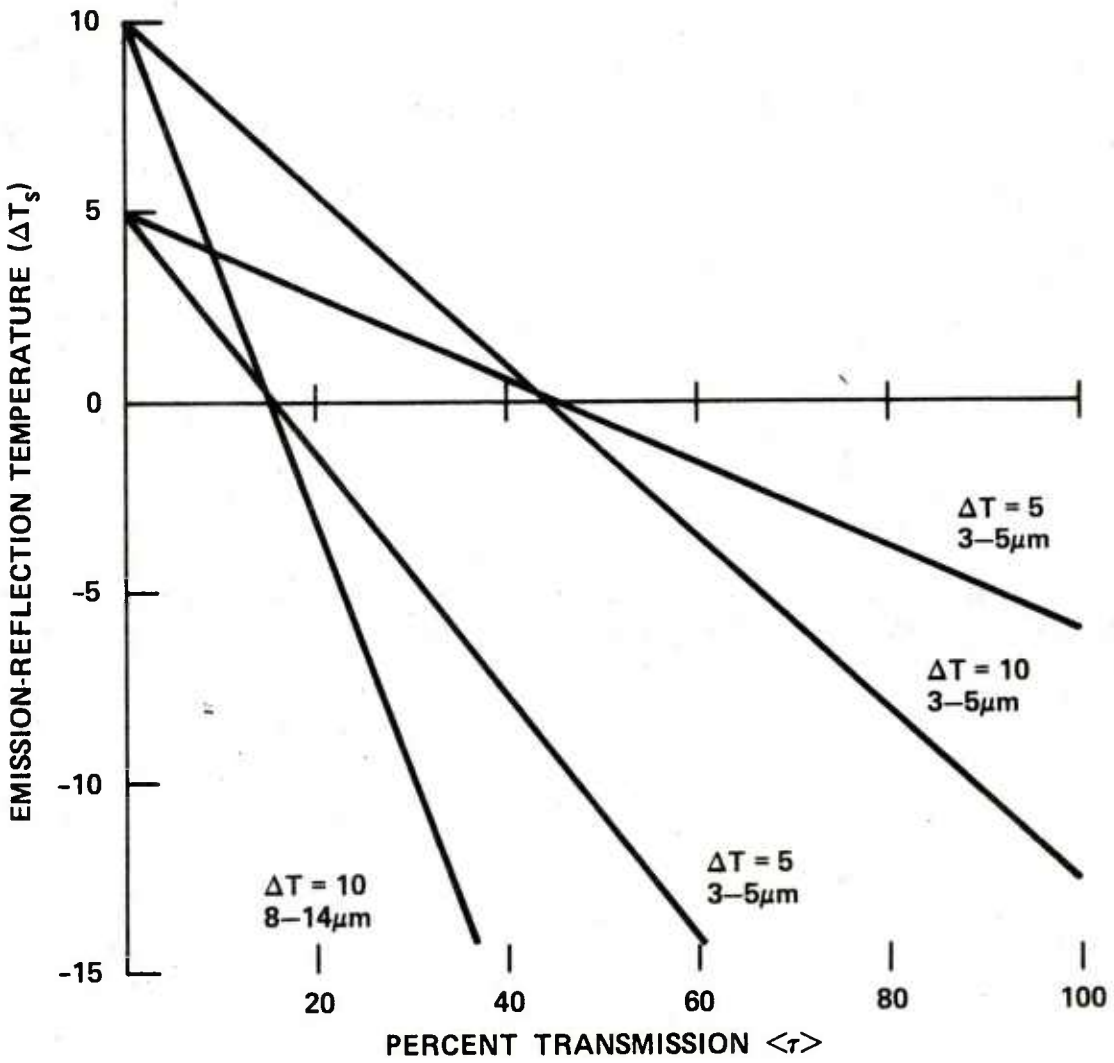
10
5
0
-5
-10
-15
EMISSION-REFLECTION TEMPERATURE (ΔT_s)
ΔT = 5
3–5μm
ΔT = 10
3–5μm
ΔT = 5
3–5μm
ΔT = 10
8–14μm
20
40
60
80
100
PERCENT TRANSMISSION <τ>
Figure 18. Required Emission-Reflection Temperature Necessary to Saturate a Thermal Imaging System (Case B)

CASE C. The relationship between emission-reflection and attenuation causes the image to disappear into a gray level and then the entire screen will be gray. Then

$$I_{ST} - I_{SB} \leq \frac{I_{OT} - I_{OB}}{10} \tag{29}$$

where

$$I_{OB} \leq I_{SB}$$

$$I_{ST} \leq I_{OT}$$

Comparing this to equation 16, we see that

$$\langle \tau \rangle \leq \frac{1}{10} \tag{30}$$

This is an unexpected result! It indicates that the observer will be unable to see his target every time the spectral averaged transmission drops below 10% for a 10 gray level system provided that he does not readjust his thermal imaging system. If the system is not optimized, i.e., both the background and target are in the gray levels, then the relationship presented above is relaxed in the sense that a higher transmission smoke will produce the same effect. Thus, the three cases presented are "worst" cases.

Consider, now, the device which has an AGC or one that is readjusted for optimum display after the smoke is present. The only inequality that exists is when the attenuation and emission-reflection combined produces a signal differential between the target and background that is below the equivalent noise.

$$I_{ST} - I_{SB} \leq I_N \tag{31}$$

If we represent this current as an equivalent blackbody R_N with emissivity $\epsilon = 1$, then

$$\int S\tau_s\tau_a(\epsilon_T R_T - \epsilon_B R_B)d\lambda \leq \int S R_N d\lambda \tag{32}$$

The equivalent input noise is defined as a small increment about the background temperature so that

$$R_N = a\, \Delta T_N\, R_B \tag{33}$$

Note that R_N is defined in the laboratory and, therefore, the atmospheric transmission does not appear in the right-hand side of equation 33. If $\epsilon_T = \epsilon_B = 1$, then

$$\int S\tau_s\tau_a d\lambda = \langle\tau_s''\rangle \leqslant \frac{\Delta T_N}{\Delta T} \tag{34}$$

which is the well-known equation that indicates the spectral average smoke transmission must be sufficiently small to reduce the target-background differential below the MRT of the imaging system. Note also that this average $\langle\tau''\rangle$ is different from that defined by equation 19.

For both systems (e.g., with AGC and without), we have assumed that the emissivities were equal to one in several places and that the blackbody flux was wavelength independent and proportional only to the temperature. These assumptions permitted us to plot certain parameters and to draw certain conclusions. In practice, however, none of the assumptions are truly valid, and, therefore, we must consider the conclusions as guidelines rather than as facts.

Because of all the problems associated with thermal imaging systems, they should not be used to quantify the effectiveness of smoke. Rather they should be used solely for qualitative purposes.

VII. THERMAL CLUTTER.

Thermal clutter is defined as many hot sources within the thermal imaging system's FOV that will confuse the observer so that he will be unable to locate the true target. The emissive properties, as well as the angular subtense required of each individual source, are not known at all. Within a smoke, natural wind velocity and diffusion can move these spots so that the observer will see only randomly moving speckles on the screen. Some of the hot spots should probably be at least the size of the target. Pattern recognition studies may suggest the size, temperature, and number of local hot spots required. It is unknown how these hot spots may be generated.

It has been shown in previous sections that a uniform emissive-reflective cloud only adds a dc component to the detected flux. The electronics are capable of eliminating this shift and, therefore, the target will be discernible within the limitations already mentioned. It was assumed that the system was adjusted so that the target was pure white and the background was pure black. In some systems, the device locates the hottest portion of the scene (presumably the target) and the coldest portion (presumably the background) and inserts the 10 gray levels in between. If the emission is sufficiently high, the detector-electronics will saturate causing either a portion or the entire display to bloom. Consider, now, a situation where a portion of a hot cloud or decoy is within the FOV. If the detector does not saturate and if the hot area is only in front of the background and not in front of the target, then the pure white level is given by

$$\int S(\tau_a' R_s + L_a' + \tau_s\tau_a\epsilon_B R_B)d\lambda \tag{35}$$

and the pure black level is given by

$$\int S(\tau_a \epsilon_B R_B + L_a) d\lambda \tag{36}$$

If 10 gray levels are introduced between the white and black levels, then the target will disappear into a gray level when

$$\int S\tau_a(\epsilon_T R_T - \epsilon_B R_B) d\lambda \leq \frac{1}{10} \int S(\tau_a' R_s + L_a' + \tau_s \tau_a \epsilon_B R_B - \tau_a \epsilon_B R_B - L_a) d\lambda \tag{37}$$

If $L_a' \approx L_a$, $\epsilon_T = \epsilon_B - 1$, $\tau_a' \approx \tau_a$, the cloud has an emissivity ϵ_s, reflection can be neglected, and the cloud is ΔT_s above ambient, then

$$\Delta T_s \geq \frac{1}{a\epsilon_s} \left[10a\, \Delta T + 1 - \langle \tau \rangle - \epsilon_s \right] \tag{38}$$

In the limit as the smoke becomes extremely dense, $\langle \tau \rangle \rightarrow 0$ and $\epsilon_s \rightarrow 1$ then

$$\Delta T_s \geq 10\, \Delta T \tag{39}$$

which is an intuitive result. The smoke temperature differential above the background must be at least ten times the target differential for the target to disappear into a gray level. This is what can happen when a hot cloud starts to drift into the FOV of a thermal imaging system.

VIII. CONCLUSIONS.

The various difficulties encountered in measuring transmission of aerosols have been discussed. Specifically, scattered light, whether single or multiple, can enter a large FOV detector and give an artificially high transmission. The size distribution of an aerosol is also directly related to the transmission. Any dynamic process, such as sedimentation and coagulation, can alter the distribution and thereby alter the extinction measurements. For aerosol measurements to be reproducible, it is necessary to generate exactly the same size distribution and concentration each time. A flow chart indicating possible errors in measurement for reproducible aerosols is shown in figure 19.

To intelligently analyze data from broadband detectors, the spectral components of the target, smoke, intervening atmosphere, and the detector must be known. To obtain consistent results, in addition to the aerosol reproducibility requirements, the target temperature and intervening atmosphere must always be the same. For small pathlengths, the atmospheric transmission is near 100%; however, for long pathlengths, the transmission depends upon relative

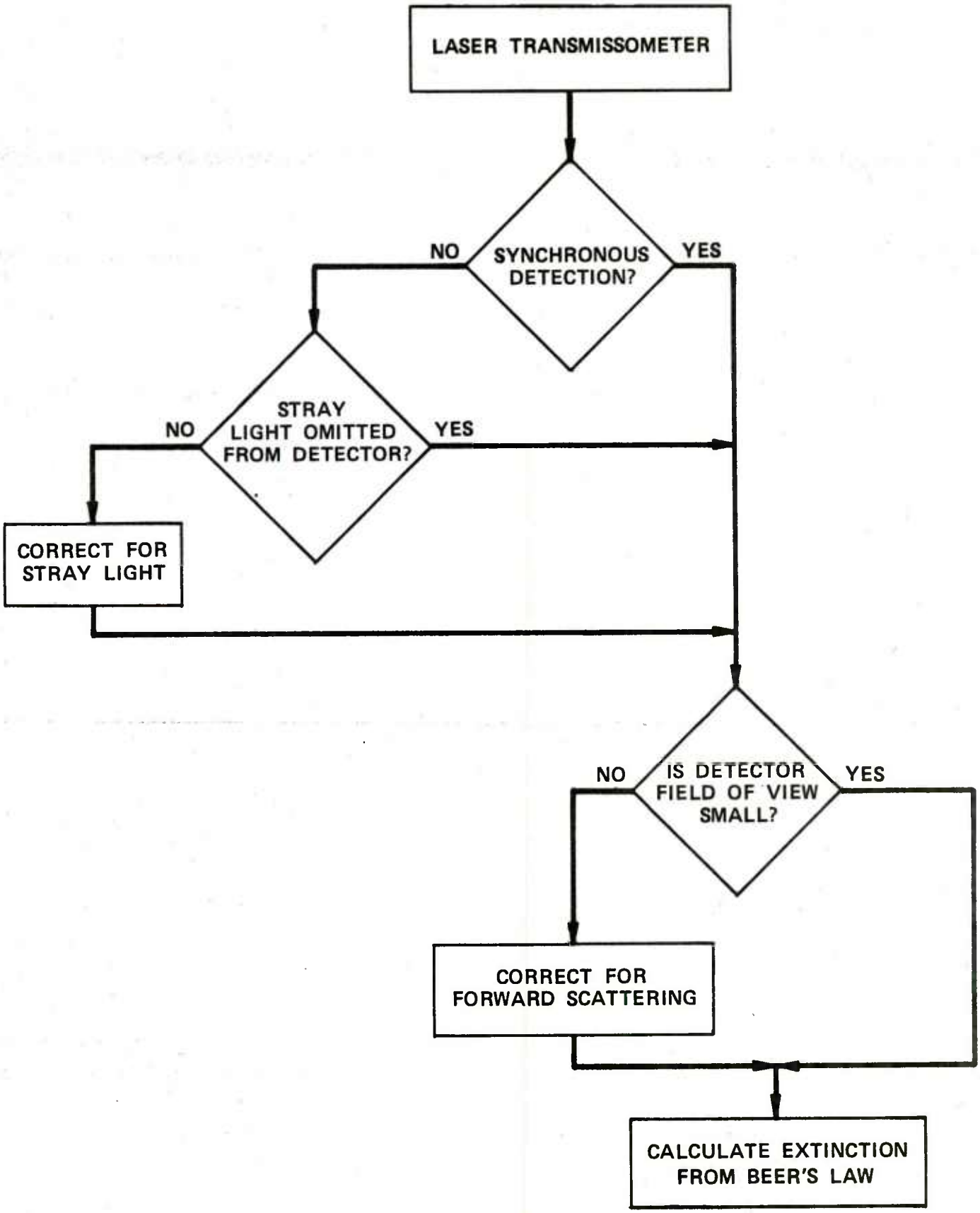

Figure 19. Flow Chart of Possible Experimental Errors Encountered with Laser Transmissometers

humidity, temperature, and atmospheric constituents, all of which can vary on an hourly basis. If two different detectors are used, the spectral responses must be identical. The flow chart illustrating these problems is shown in figure 20.

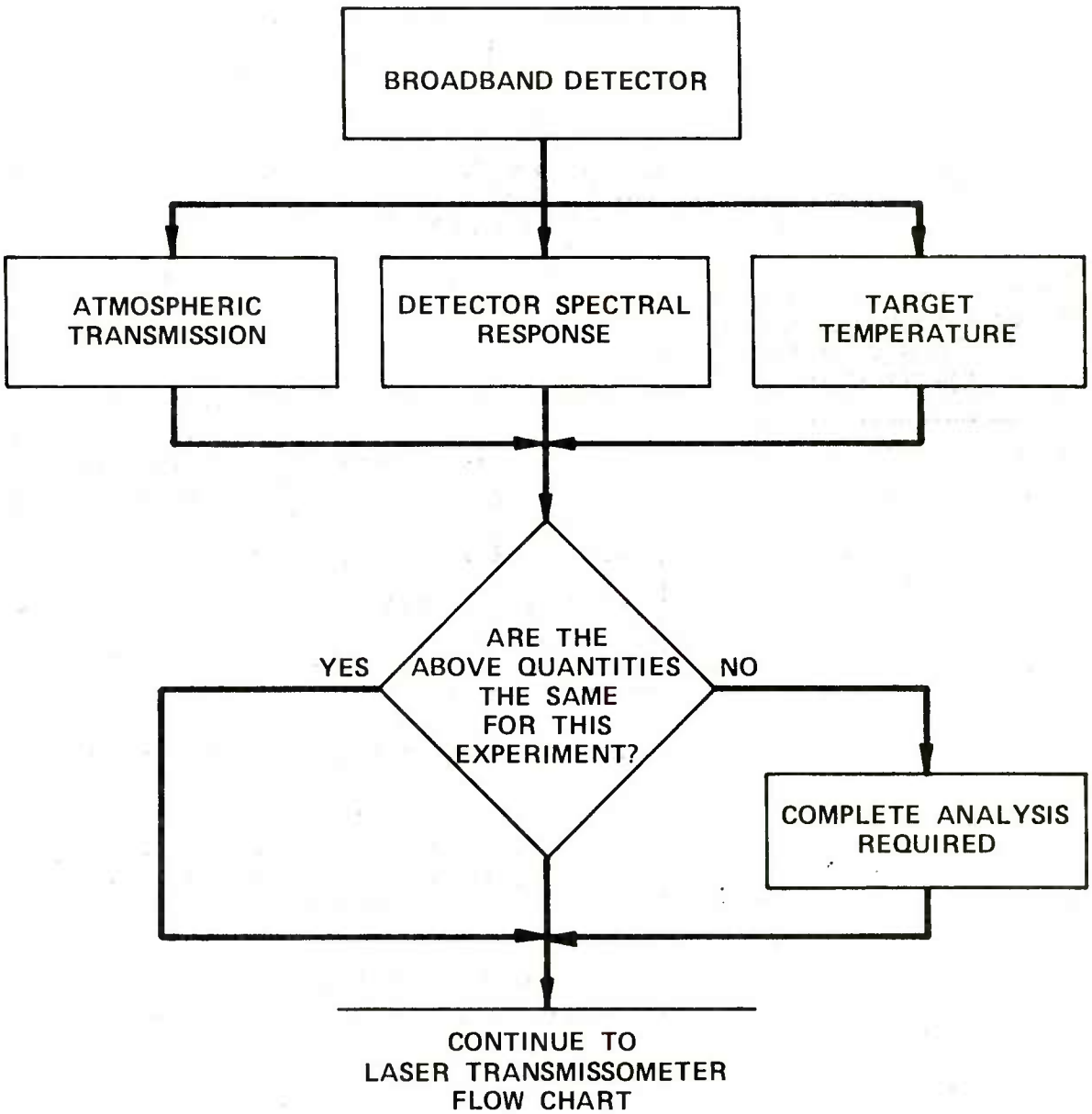

Figure 20. Flow Chart of Possible Experimental Errors Encountered with Broadband Detectors

Finally, for target obscuration with a thermal imaging system with an AGC, sufficient smoke must be present to reduce the target-background temperature differential below the MRT of the system. The MRT depends upon the angular subtense of the target. The problems inherent to broadband detectors and transmissometers also apply. The flow chart is shown in figure 21. Note that only trained observers should be used if the only information available is the display screen.

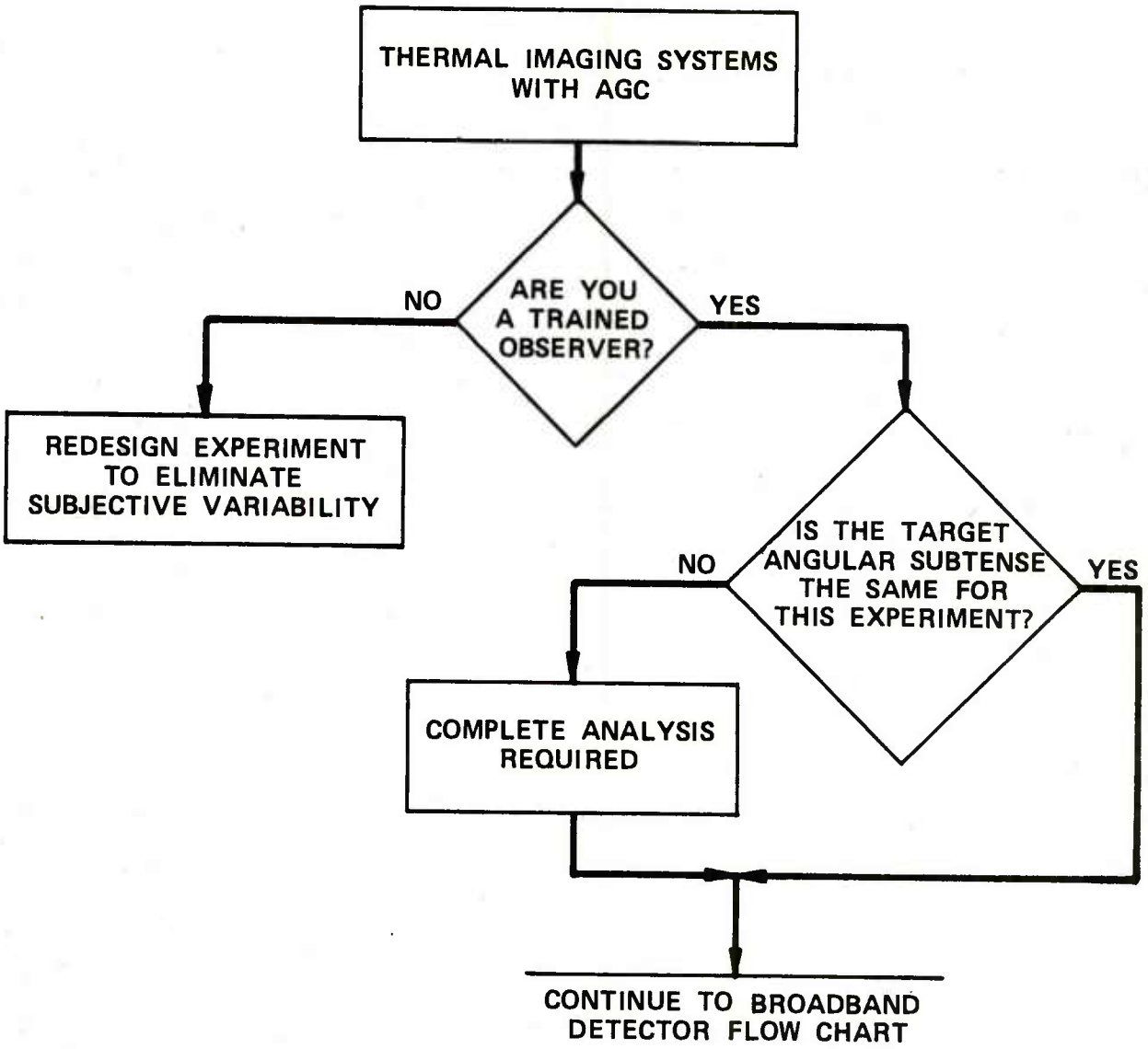

Figure 21. Flow Chart of Possible Experimental Errors Encountered with Thermal Imaging Systems

LITERATURE CITED

1. Middleton, W.E.K. Vision Through the Atmosphere. University of Toronto Press, Toronto, Canada. p 177. 1952.

2. Zuev, V. E., Kabanoo, M. V., and Savelev, B. A. Propagation of Laser Beams in Scattering Media. Applied Optics *8*, 137 (1969).

3. Deepak, A., and Box, M. A. Forward Scattering Corrections for Optical Extinction Measurements in Homogeneous Polydisperse Aerosols. *Ibid. 17*, 3169 (1978).

4. Handbook on Aerosols. R. Dennis, Editor, GCA Corporation, Bedford, Massachusetts. Prepared for U.S. Energy Research and Development Administration. 1976. [Copies are available from National Technical Information Service, Springfield, Virginia 22161.]

5. Mooradian, G. C., Geller, M., Stotts, L. B., Stephens, D. H., and Krautwald, R. A. Blue-green Pulsed Propagation Through Fog. Applied Optics *18*, 429 (1979).

6. Eloranta, E. W. Calculation of Doubly Scattered Lidar Returns. Ph.D. Thesis. University of Wisconsin. 1972.

7. Ryan, J. S., Pal, S. R., and Carswell, A. I. Laser Backscattering from Dense Water Droplet Clouds. Journal of the Optical Society of America *69*, 60 (1979).

8. Milham, M. ED-SP-77002. A Catalog of Optical Extinction Data for Various Aerosol/Smokes. June 1976.

APPENDIX A

EXAMINATION OF THE CORRELATION BETWEEN LABORATORY AND FIELD SMOKE EXTINCTION DATA

G. C. Holst
M. E. Milham
Chemical Systems Laboratory
Research Division
Aberdeen Proving Ground, Maryland

I. INTRODUCTION.

When lasers or narrow bandwidth detectors are used to obtain extinction coefficients of various smokes, there exists reasonable agreement between laboratory and field measurements. However, when broadband detectors are used, the measured integrated transmission depends upon the spectral transmission of the smoke, target emissive characteristics, detector spectral response, and the atmosphere spectral transmission. The back calculation to extinction coefficient from transmission data can lead to any arbitrary result. Thus, with knowledge of the relationship among the various parameters, one can "prove" that the extinction coefficient is almost any prechosen value by judiciously selecting a detector with the appropriate spectral response and a target of the appropriate temperature.

The detected signal is given by

$$V = \int T_A R_T S T_S d\lambda \tag{A-1}$$

where

T_A = atmospheric transmission

R_T = energy emitted by the target

T_S = smoke transmission

S = spectral response of the sensor

and the integration is taken over the wavelength region of interest. In general, all parameters are a function of wavelength. During experiments, the usual measurement is to ratio the signal with smoke to that without smoke and call this ratio the transmission. This is represented as

$$T = \frac{\int T_A R_T S T_S d\lambda}{\int T_A R_T S d\lambda} \tag{A-2}$$

If the smoke has no spectral absorption (e.g., the transmission is independent of wavelength), then T_S can be taken out of the integral so that $T=T_S$ which is the desired result. With narrow band detectors or lasers, the wavelength region is so small that $T=T_S$.

Given the transmission, it is tempting to infer an extinction coefficient a, by using Beer's law

$$a = \frac{1}{CL} \ln \frac{1}{T} \qquad \text{(A-3)}$$

where

C = concentration

L = pathlength

It has been previously shown[1] that the effective extinction coefficient (back calculated from transmission and CL values) is a function of the target temperature and sensor response. Those calculations were obtained for typical 3- to 5- and 8- to 12-μm detectors.

The present work compares field data obtained at Dugway Proving Ground during Smoke Week I with theoretical calculations. These calculations include the actual sensor system and target temperature used at Dugway Proving Ground. Furthermore, the atmospheric transmission using LOWTRAN 4 has been included.

II. CALCULATIONS.

The spectral extinction coefficient of white phosphorus (WP) obtained in the laboratory is shown in figure A-1.[2] To illustrate the effect of spectral extinction, the transmission of WP with a 600-m atmospheric pathlength is plotted in figure A-2 as a function of CL. It is readily apparent from this figure that since broadband detectors integrate under the curve, different spectral response will yield different total transmissions. Using equation A-2, the transmission of several commercially available detectors has been calculated (table A-1).

It is precisely the fact that the transmission is very high in the 11- to 13-μm region that it was suggested that CO_2 isotope lasers should be considered.[3] The expected laser transmission for WP is given in table A-2.

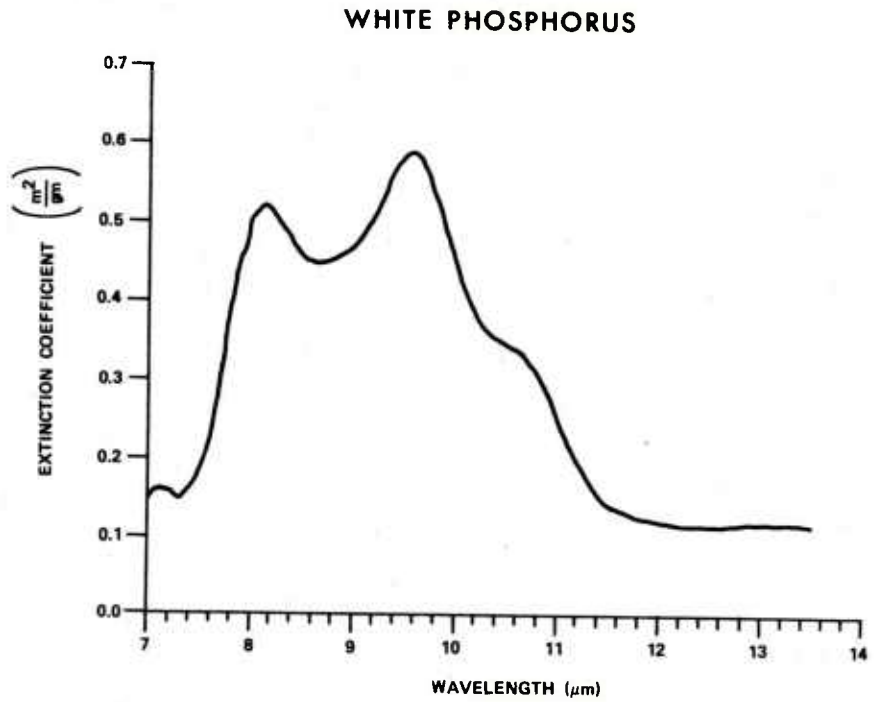

Figure A-1. Spectral Extinction Coefficient of WP

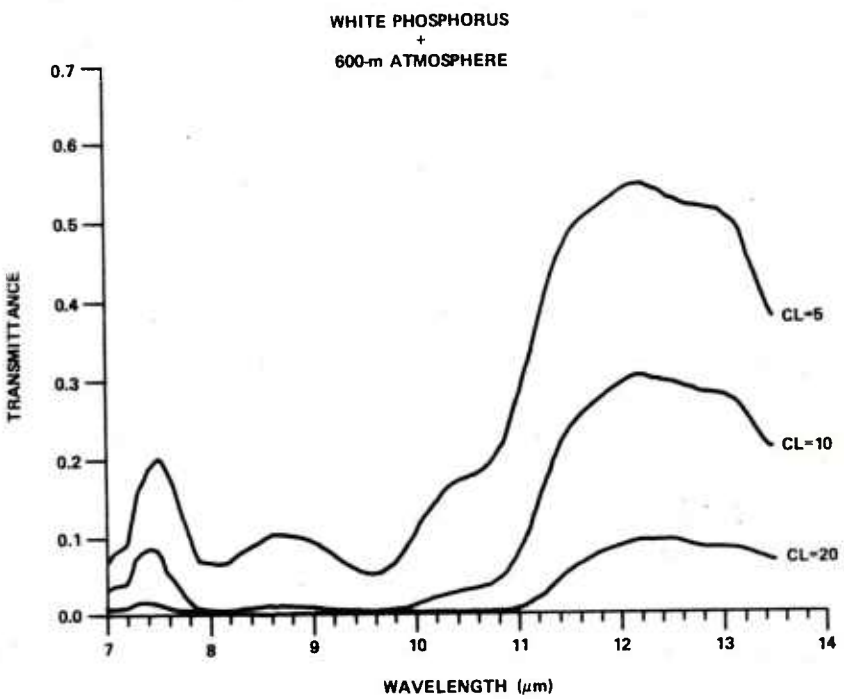

Figure A-2. Spectral Transmission of WP for Various CL Values

(Atmospheric pathlength, 600 m)

Table A-1. Calculated Transmission of WP Smoke Using Various Detectors

Detector	CL = 5	CL = 10
	%	
Infrared associates HgCdTe	31	14
Barnes immersed thermistor	26	10
Barnes pyroelectric	30	13
Barnes HgCdTe	31	14
Honeywell HgCdTe	25	9

Table A-2. Transmission of Various CO_2 Laser Lines in WP

CO_2 laser line	CL = 5	CL = 10
μm	%	
9.6	7.4	.55
10.6	19	3.6
11.2	40	16
11.8	52	27

Now that the problems associated with broadband detectors have been identified, consider Dugway Proving Ground test trial DP1-002-T23, 6 October 1977.[4] The munition was a 155-mm WP round. This test produced CL values up to 27. The atmospheric conditions of 6 October 1977 were inputted to the LOWTRAN code to obtain the atmospheric transmission. Detector response curves (bolometer) and filter transmission curves (7.63 - 11.37 μm) were obtained from Dugway Proving Ground. The source was an 1800°K blackbody. The effective extinction coefficient was back calculated using equations A-2 and A-3 by first assuming a CL value and then calculating α. A plot was generated for all values of CL (figure A-3). The actual Dugway Proving Ground data are also plotted in figure A-3 where the transmission from the "9.75-μm" filter and the actual CL values obtained from the aerosol photometers were used to calculate an effective extinction coefficient.

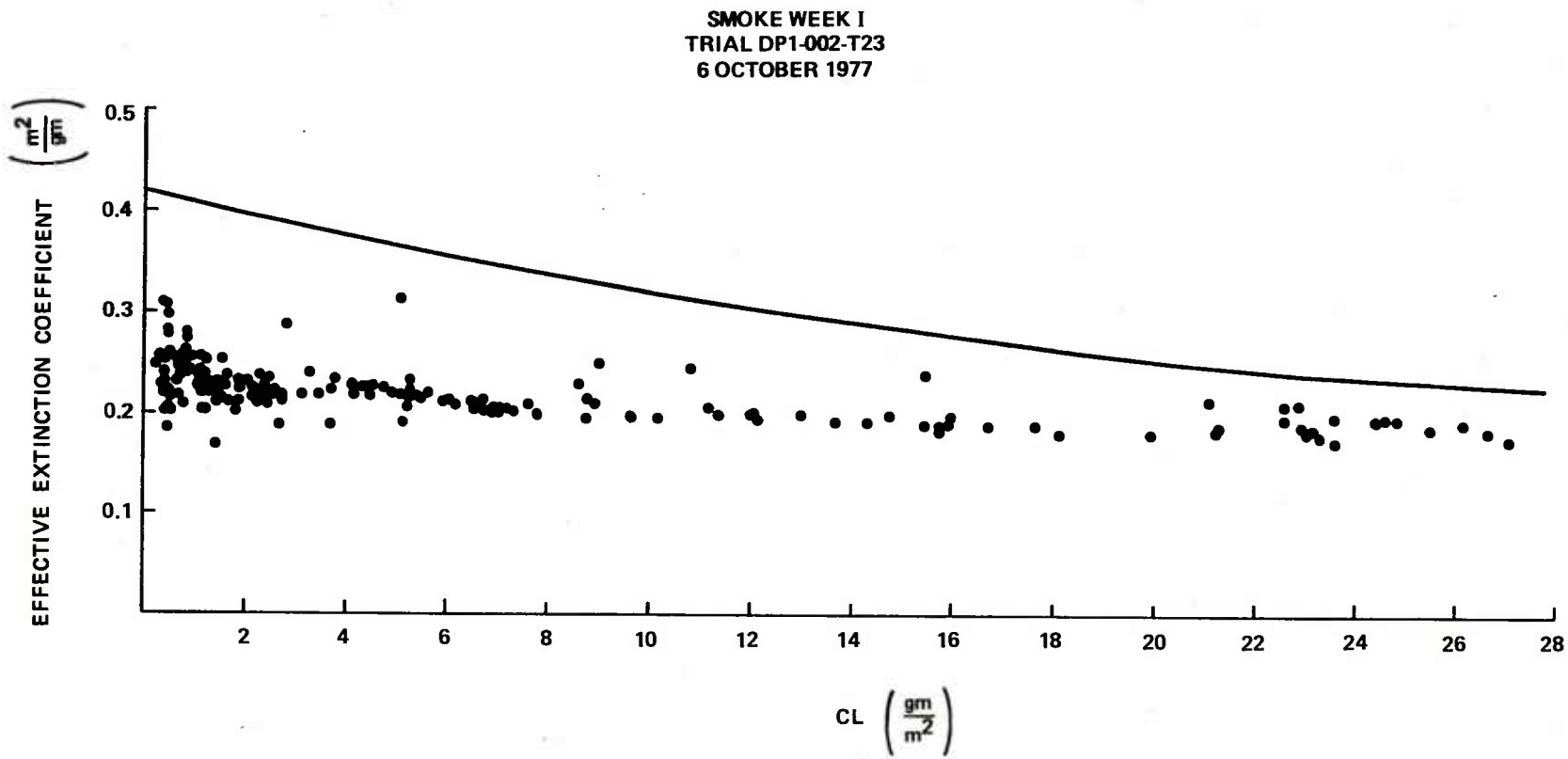

Figure A-3. Calculated (Solid Line) and Experimental (Dots) Values of Effective Extinction Coefficient for the "9.75-μm" Detector as a Function of CL

III. DISCUSSION.

The fact that the effective extinction decreases as CL increases is a result of the fact that a broadband detector is not ideal when smokes exhibit spectral character. If the smoke had constant transmission as a function of wavelength, then a would be independent of CL. As a further check on the sensitivity of a to spectrally absorbing smokes, calculations were performed on lamp black. As seen in figure A-4, lamp black has a very small change in a as a function of wavelength. It may be loosely said that it is essentially independent of wavelength when compared to WP. The results of these calculations are shown in figure A-5. We see that even with this slight change in a there is also a dependency of apparent extinction upon CL.

The experimental and theoretical curves in figure A-3 are quite similar in shape but differ by a constant factor. The fact that the curves are similar in shape supports the methodology used to calculate the extinction coefficient. There are several possible causes for the absolute difference. The first most likely is that the laboratory measurements were not calibrated properly. However, recent independent laboratory data[5] obtained with a fast scanning Michelson interferometer agree quite well with Chemical Systems Laboratory data. The second most likely cause may be the method by which Dugway Proving Ground obtains extinction coefficients. Their method[6] requires knowledge of the yield factor; whereas, the laboratory method does not.

It is known that, when phosphorus is oxidized, it does not immediately hydrate to orthophosphoric acid.[2] Therefore, the theoretical yield factor[7] which applies only to orthophosphoric acid may be as much as a factor of two higher than the yield factor obtained when phosphorus is initially hydrated into various metaphosphoric and tetrametaphosphoric acids. Although the yield factor has not been definitively researched, laboratory yield factors are much lower than the theoretical limits. If a lower yield factor were used by Dugway Proving Ground, then there would be excellent laboratory-field agreement.

If the detector's bandwidth was small and near the edge of transmission (e.g., 7 to 8 μm), then the atmosphere would significantly affect the measured transmission. For the detector-filter combination used by Dugway Proving Ground, calculations show that different environments (hot dry versus cold damp) do not appreciably affect the measured transmission.

IV. CONCLUSION AND RECOMMENDATION.

Broadband detectors are not ideal when measuring transmission of smokes unless the detector used exactly matches a fieldable device such as a forward looking infrared system. Because of the dependence of the extinction coefficient on CL, ratios should not be employed when comparing data at various wavelengths.

The yield factor can significantly affect the Dugway Proving Ground method of obtaining extinction coefficients. It is recommended that a definitive experiment be carried out to identify each intermediate phosphoric acid species and to determine the yield factor. Since the species evolve in time, the yield factor is probably a function of time.

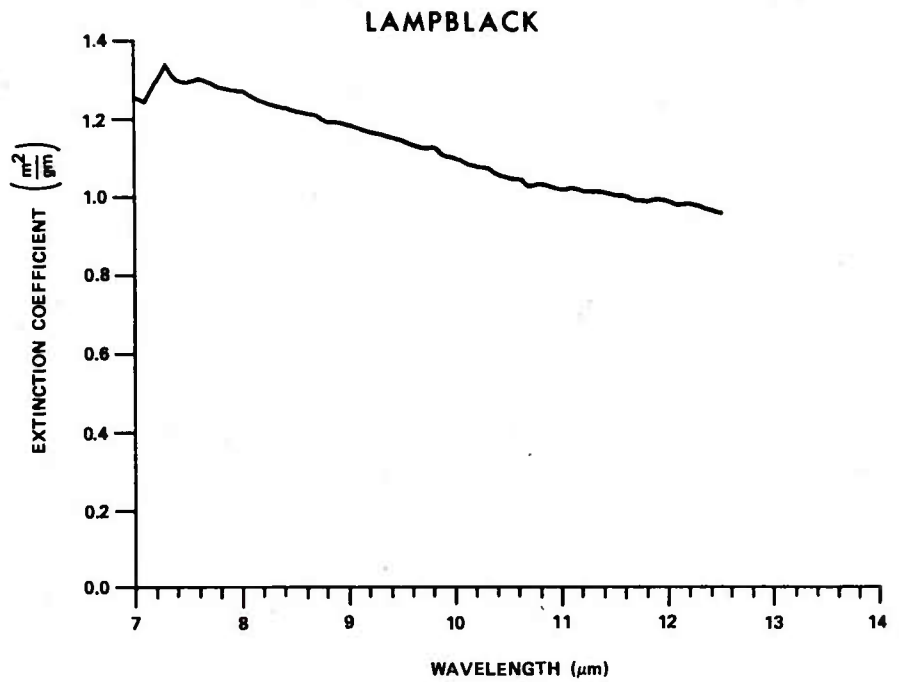

Figure A-4. Spectral Extinction Coefficient of Lampblack

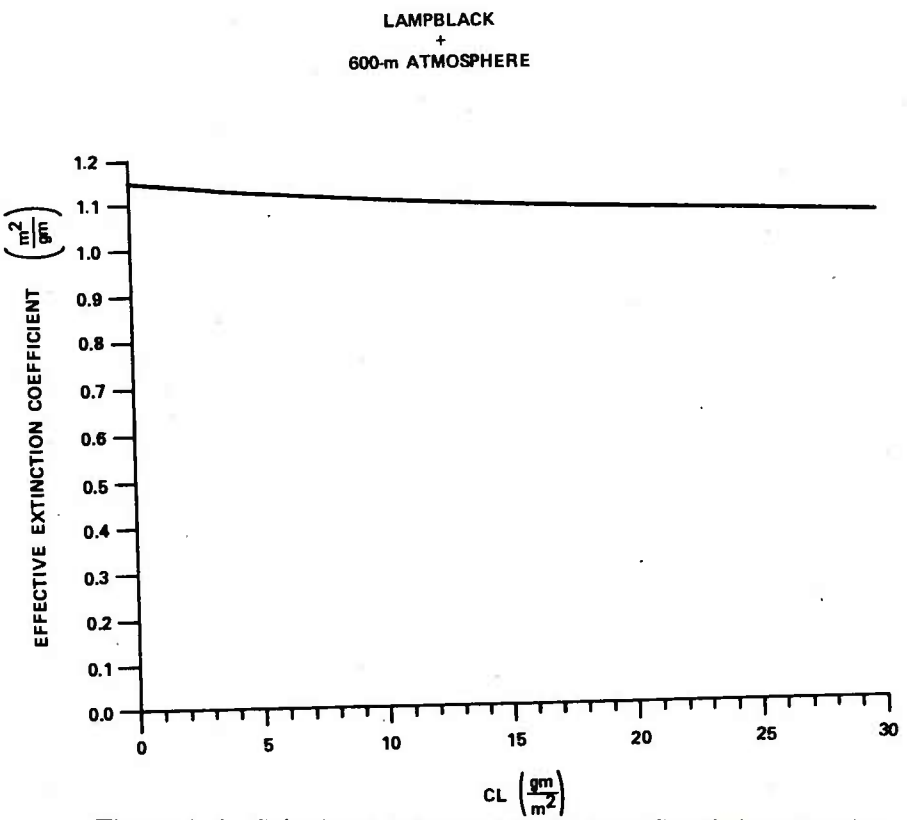

Figure A-5. Calculated Effective Extinction Coefficient for the "9.75-μm" Detector as a Function of CL

LITERATURE CITED

1. Stuebing, E. W. Deviations from Beer's Law Which Sometimes Prevent Defining a Single Overall Extinction Coefficient for a Smoke in Each Atmospheric Window. Presented at Smoke Symposium II, Harry Diamond Laboratories, April 1978.

2. Milham, M. E., Anderson, D. H., Frickel, R. H., and Tarnove, T. L. ARCSL-TR-77067. New Findings on the Nature of WP/RP Smokes. July 1977.

3. Rhode, R. S., and Papayoanou, A. Transmission of 11-12 Micron CO_2 Laser Radiation Through Battlefield Smokes. Presented at Smoke Symposium II, Harry Diamond Laboratories, April 1978.

4. Inventory Smoke Munition Test. DPG-FR-77-314. Final Test Report. June 1978.

5. Spectral Mass Extinction Coefficients of Phosphoric Acid Smokes (RP) in the 3.0 to 12.5 μm Infrared Range. Bundesinstitut fur chemisch-technische Untersuchungen (BICT) (Federal Chemical Engineering Institute), Swistall, FRG. Interim Report. 1 March 1978. Ref. No. 3.2-3/4474/78.

6. Methodology Investigation for Testing Effectiveness of Smoke/Aerosol Munitions, Pilot Study. DPG-FR-76-701. Final Report. October 1977.

7. Rubel, G. O. ARCSL-TR-78057. Predicting the Droplet Size and Yield Factors of a Phosphorus Smoke as a Function of Droplet Composition and Ambient Relative Humidity under Tactical Conditions. November 1978.

APPENDIX B

LINEARIZATION OF THE BLACKBODY CURVE

As was mentioned in section IV and shown in figure 14, the output of a broadband imaging system is calibrated against the temperature of the blackbody source. The detector, however, is sensitive to the flux rather than the temperature. The flux is given by Planck's law

$$R(\lambda,T) = K\lambda^{-5}[EXP(B/\lambda T) - 1]^{-1} \qquad \text{B-1}$$

where K = constant, B = 14388 $\mu m \cdot {}^{\circ}K$, λ = wavelength, and T = the temperature. With the Wien approximation, it can readily be shown that the first two terms of the Taylor series expansion are

$$R(\lambda,T) \approx R(\lambda_0,T_0)\left[1 + \frac{B}{\lambda_0 T_0^2}\Delta T\right] \qquad \text{(B-2)}$$

where T_0 is the background temperature taken as $T_0 = 293^{\circ}K$, λ_0 is a wavelength midpoint within the spectral range [$\lambda_0 = 4\ \mu m$ for the 3- to 5-μm range, and $\lambda_0 = 11\ \mu m$ for the 8- to 14-μm range], and $T_0 + \Delta T$ is the temperature of the source. Therefore, in this representation, ΔT is the target-background temperature differential. R(λ,T) is independent of wavelength and is a function of only ΔT.

The error associated with this expansion is given as

$$E = 1 - \frac{R(\lambda_0,T_0)\left(1 + \frac{B}{\lambda_0 T_0^2}\Delta T\right)}{R(\lambda,T)} \qquad \text{(B-3)}$$

and is shown in figure B-1. The errors associated with the 3- to 5-μm region are extremely large suggesting that this representation is not valid.

The reason that thermal imaging systems can be linearized is that the output is integrated over the entire spectral range. There are equal positive errors and negative errors in the Taylor series expansion and these tend to cancel. To prove that this is so, the intensity

$$I = \int SR d\lambda \qquad \text{(B-4)}$$

was calculated using equation B-1 (the exact solution) and with equation B-2 (the approximate solution) for a typical InAs (3- to 5-μm) detector and for a typical HgCdTe (8- to 14-μm) detector. The relative intensities are shown in figure B-2. Thus the integrated output is proportional to ΔT.

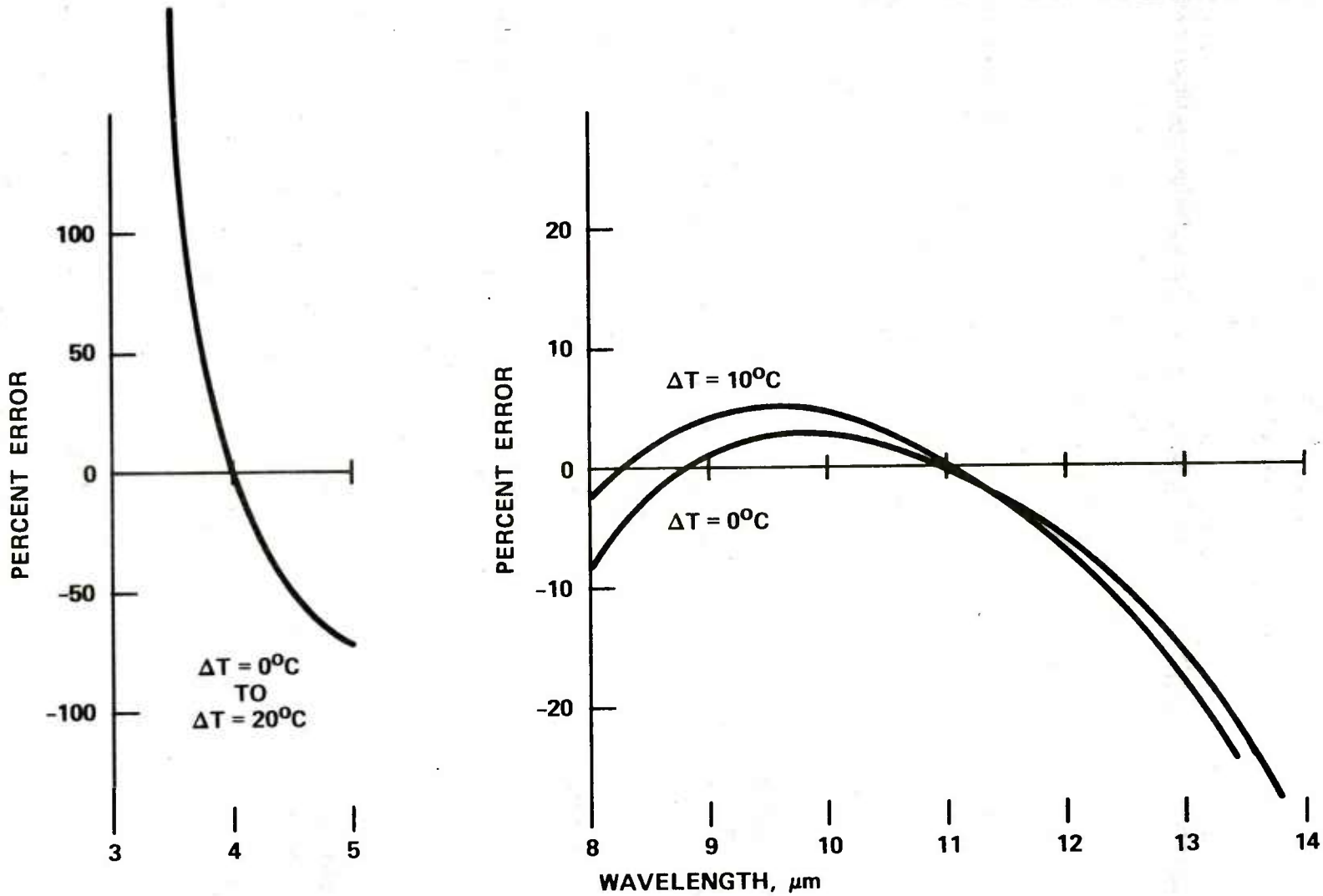

Figure B-1. Percent Error Calculated for Two Spectral Regions When Using the Linearization Approximation

Note the different ordinate scales.

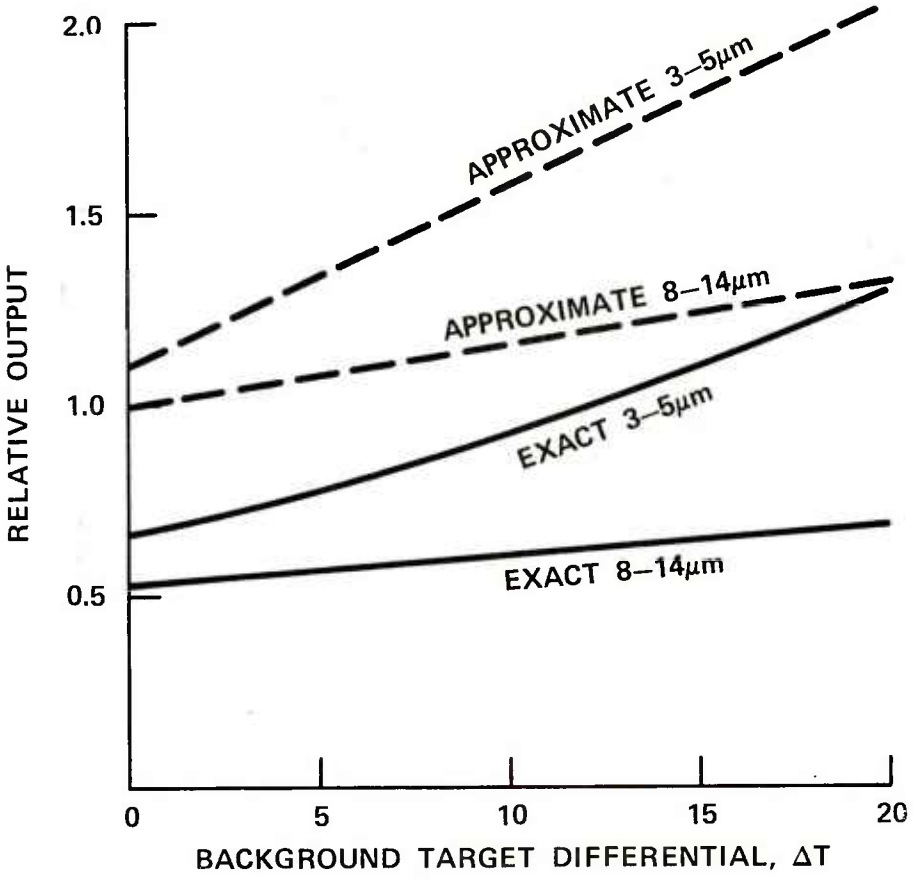

Figure B-2. Relative Output of Two Detectors in Two Spectral Ranges

The outputs have been scaled to show the linearity between output and ΔT.

DISTRIBUTION LIST 6

Names	Copies
CHEMICAL SYSTEMS LABORATORY	
SAFETY OFFICE	
Attn: DRDAR-CLF	I
AUTHOR'S COPIES: Research Division	50
USA BIOMEDICAL LABORATORY	
Attn: SGRD-UV	1
DEVELOPMENTAL SUPPORT DIVISION	
Attn: DRDAR-CLJ-R	3
Attn: DRDAR-CLJ-L	3
Attn: DRDAR-CLJ-M	1
Attn: DRDAR-CLJ-P	1
MUNITIONS DIVISION	
Attn: DRDAR-CLN	5
RESEARCH DIVISION	
Attn: DRDAR-CLB	1
Attn: DRDAR-CLB-B	1
Attn: DRDAR-CLB-C	1
Attn: DRDAR-CLB-P	1
Attn: DRDAR-CLB-R	1
Attn: DRDAR-CLB-T	1
Attn: DRDAR-CLB-TE	1
SYSTEMS DEVELOPMENT DIVISION	
Attn: DRDAR-CLY-A	1
Attn: DRDAR-CLY-R	6
DEPARTMENT OF DEFENSE	
Defense Technical Information Center Attn: DTIC-DDA-2 Cameron Station, Bldg. 5 Alexandria, VA 22314	12
Director Defense Intelligence Agency Attn: DB-4G1 Washington, DC 20301	1
DEPARTMENT OF THE ARMY	
HQDA (DAMO-SSC) WASH DC 20310	1
Director Defense Civil Preparedness Agency Attn: PO(DC) Washington, DC 20301	1
CINCUSAREUR Attn: AEAGC-RSI APO New York 09403	1
Deputy Chief of Staff for Research, Development & Acquisition	
Attn: DAMA-CSM-CM	1
Attn: DAMA-ARZ-D Washington, DC 20310	1

Names	Copies
US Army Research and Standardization Group (Europe) Attn: Chief, Chemistry Branch Box 65, FPO New York 09510	1
HQDA (DAMI-FIT) WASH, DC 20310	I
Commander HQ US Army Medical Command, Europe Attn: AEMPM APO New York 09403	I
US ARMY HEALTH SERVICE COMMAND	
Superintendent Academy of Health Sciences US Army	
Attn: HSA-CDC	1
Attn: HSA-IHE Fort Sam Houston, TX 78234	I
US ARMY MATERIEL DEVELOPMENT AND READINESS COMMAND	
Commander US Army Materiel Development and Readiness Command	
Attn: DRCLDC	1
Attn: DRCSF-P 5001 Eisenhower Ave Alexandria, VA 22333	1
Commander US Army Toxic & Hazardous Materials Agency Attn: DRXTH-TS Aberdeen Proving Ground, MD 21010	2
Project Manager Smoke/Obscurance Attn: DRCPM-SMK-M Aberdeen Proving Ground, MD 21005	1
Human Engineering Laboratory HFE Detachment Attn: DRXHE-APG Building 520 Aberdeen Proving Ground, MD 21005	1
Commander US Army Foreign Science & Technology Center Attn: DRXST-MT3 220 Seventh St., NE Charlottesville, VA 22901	1
US Army Materiel Systems Analysis Activity	
Attn: DRXSY-MP	1
Attn: DRXSY-T (Mr. Kaste) Aberdeen Proving Ground, MD 21005	1
Director DARCOM Field Safety Activity Attn: DRXOS-C Charlestown, IN 47111	1

DISTRIBUTION LIST 6 (Contd)

Names	Copies
Commander	
US Army Armament Research and Development Command	
Attn: DRDAR-AC	1
Attn: DRDAR-LCA	1
Attn: DRDAR-LCU	1
Attn: DRDAR-SCA-C	1
Attn: DRDAR-SCP-A	1
Attn: DRDAR-SCW	1
Attn: DRDAR-SER	1
Attn: DRDAR-TSS	2
Dover, NJ 07801	
Commander	
Armament Concepts Office, Weapon Systems Concepts Team	
Attn: DRDAR-ACW	1
Aberdeen Proving Ground, MD 21010	
Director	
Ballistic Research Laboratory	
Attn: DRDAR-TSB-S	2
Building 305	
Aberdeen Proving Ground, MD 21005	
CDR, APG	
USA ARRADCOM	
Attn: DRDAR-GCL	1
Aberdeen Proving Ground, MD 21010	
US ARMY ARMAMENT MATERIEL READINESS COMMAND	
Commander	
US Army Armament Materiel Readiness Command	
Attn: DRSAR-LE	1
Attn: DRSAR-PDM	1
Attn: DRSAR-SA	1
Attn: DRSAR-SF	1
Rock Island, IL 61299	
CDR, APG	
USA ARRCOM	
Attn: SARTE	1
Aberdeen Proving Ground, MD 21010	
Commander	
US Army Dugway Proving Ground	
Attn: Technical Library, Docu Sect	1
Dugway, UT 84022	
Commander	
Rocky Mountain Arsenal	
Attn: SARRM-QA	1
Commerce City, CO 80022	
Commander	
Pine Bluff Arsenal	
Attn: SARPB-ETA	1
Pine Bluff, AR 71611	

Names	Copies
US ARMY TRAINING & DOCTRINE COMMAND	
Commandant	
US Army Infantry School	
Attn: NBC Division	1
Fort Benning, GA 31905	
Commandant	
US Army Missile & Munitions Center & School	
Attn: ATSK-CD-MD	1
Attn: ATSK-DT-MU-EOD	1
Redstone Arsenal, AL 35809	
Commandant	
US Army Military Police School/Training Center	
Attn: ATZN-CDM	1
Attn: ATZN-TDP-C	4
Fort McClellan, AL 36205	
Commander	
US Army Infantry Center	
Attn: ATSH-CD-MS-C	1
Fort Benning, GA 31905	
Commandant	
US Army Ordnance & Chemical Center & School	
Attn: ATSL-CL-CD	1
Aberdeen Proving Ground, MD 21005	
Commander	
USA Training & Doctrine Command	
Attn: ATCD-Z	1
Fort Monroe, VA 23651	
Commander	
USA Combined Arms Combat Development Activity	
Attn: ATZLCA-CO	1
Fort Leavenworth, KS 66027	
US ARMY TEST & EVALUATION COMMAND	
Commander	
US Army Test & Evaluation Command	
Attn: DRSTE-FA	1
Aberdeen Proving Ground, MD 21005	
DEPARTMENT OF THE NAVY	
Commander	
Naval Explosive Ordnance Disposal Facility	
Attn: Army Chemical Officer, Code 604	1
Indian Head, MD 20640	
Commander	
Nuclear Weapons Training Group, Atlantic	
Naval Air Station	
Attn: Code 21	1
Norfolk, VA 23511	

DISTRIBUTION LIST 6 (Contd)

Names	Copies
Chief, Bureau of Medicine & Surgery Department of the Navy Washington, DC 20372	1
Commander Naval Weapons Center Attn: A. B. Galloway/Code 3171 China Lake, CA 93555	1
Commanding Officer Naval Weapons Support Center Attn: Code 5042/Dr. B. E. Douda Crane, IN 47522	1
US MARINE CORPS	
Director, Development Center Marine Corps Development & Education Command Attn: Fire Power Division Quantico, VA 22134	1
DEPARTMENT OF THE AIR FORCE	
HQ Foreign Technology Division (AFSC) Attn: PDRR Wright-Patterson AFB, OH 45433	1
Commander Aeronautical Systems Division Attn: ASD/AELD Wright-Patterson AFB, OH 45433	1
HQ, USAF/SGES Bolling AFB, DC 20332	1
HQ AFISC/SEV Norton AFB, CA 92409	1
OUTSIDE AGENCIES	
Battelle, Columbus Laboratories Attn: TACTEC 505 King Avenue Columbus, OH 43201	1
Director of Toxicology National Research Council 2101 Constitution Ave, NW Washington, DC 20418	1

Names	Copies
ADDITIONAL ADDRESSEES	
Commander USEUCOM Attn: ECJ-O/LTC James H. Alley APO, NY 09128	1